• U C •
FCTUC FACULDADE DE CIÊNCIAS
E TECNOLOGIA
UNIVERSIDADE DE COIMBRA

Daniel Costa Silva

On the evaluation of easily measured biosignals features for non-invasive and continuous arterial pressure estimation

Thesis submitted to the
University of Coimbra for the degree of
Master in Biomedical Engineering

Supervisors:

Prof. Dr. Jorge Henriques (Faculty of Sciences and technology, University of Coimbra)

Prof. Dr. César Teixeira (Faculty of Sciences and technology, University of Coimbra)

Dr. Jens Muehlsteff ("Patient Care and Measurements" research department, Philips Electronics)

Coimbra, 2017

This work was developed in collaboration with:

Philips Research and development

Politecnico di Milano

Acknowledgements

Firstly, I'd like to express my appreciation for the proposed challenging work and support by Dr. Jens Muehlsteff. Also, I'm truly grateful for the incredible opportunity to spend 4 months in Eindhoven and work in those inspiring facilities. This experience was entirely supported by Philips "Patient Care and Measurements" research group. For that, I cannot possibly thank enough.

Enormous thanks for the provided support by Professor Jorge Henriques and Professor César Teixeira throughout the entire dissertation. They had the patience to clarify any doubt I had, as many times as it was needed. That was a major contribution.

A special thank you to the group of interns with whom I shared those 4 months in Eindhoven. They contributed for the great work environment and made me feel at home even when the hagelslag was missing.

At last but not least, a final greeting to the university of Coimbra and the Physics Department for the "ZOO" of friends and experiences that I'll carry with me

Resumo

Esta dissertação pretendeu estudar e avaliar a pressão sanguínea estimada, de uma forma continua e não invasiva, a ser implantada durante cirurgias, dependendo apenas de parâmetros extraídos de modalidades não-invasivas (Fotopletismografia e Eletrocardiografia). Da Fotopletismografia, parâmetros foram extraídos através dos seus componentes pulsáteis e não-pulsáteis, assim como a segunda derivada correspondente da componente pulsátil. Nomeadamente, a Amplitude da componente pulsátil, a Amplitude da componente não-pulsátil, o *ratio* entre as amplitudes pulsáteis e não-pulsáteis, a Amplitude do nó dicrótico, o Índice de reflexão, o Intervalo de batimento cardíaco e o *ratio* entre as amplitudes da forma de onda da segunda derivada da Fotopletismografia (ondas "a" e "b"). Duas implementações diferentes do Tempo de chegada do pulso foram também calculadas (de acordo com [65] e [17]) e incluídas neste conjunto de parâmetros, o que por sua vez exigiu a consideração da Eletrocardiografia nesta experimentação. A relação entre os nove parâmetros extraídos destes dois biosinais foi quantificada em termos do desempenho da correlação com quatro outros aspetos diferentes da Pressão sanguínea: a Pressão sanguínea sistólica, a Pressão sanguínea diastólica, a Pressão do pulso e a Pressão arterial média. Esta análise destacou a forte correlação entre o *ratio* das amplitudes das ondas "a" e "b" e o Tempo de chegada do pulso (calculado em [17]), e as Pressões sistólica, diastólica e arterial média, para todos os pacientes. Os coeficientes da correlação *spearman* variaram entre 71% e 90% para o parâmetro anterior e entre 75% e 91% para o posterior. Por outro lado, o Intervalo do batimento cardíaco mostrou apenas correlações negligenciáveis com os parâmetros da pressão sanguínea. Os coeficientes da correlação de *spearman* variaram entre 4% e 58%.

Além disso, os aspetos sob investigação da Pressão sanguínea foram estimados à parte da combinação dos nove parâmetros previamente mencionados, através da modelação de regressões lineares múltiplas, para cada paciente, e confirmados de acordo com a validação cruzada "leave-one-out". Diferentes modelos foram propostos e experienciados de modo a avaliar a contribuição de quatro grandes aspetos para os parâmetros da pressão sanguínea estimada. A influência da inclusão do Tempo de chegada do pulso (e consequente utilização de sensores extra de Eletrocardiograma) e da Componente não-pulsátil da Fotopletismografia nos modelos definidos foi tida em

consideração. Os biosinais foram também segmentados e calculou-se, para cada segmento, o coeficiente da correlação de *spearman* entre os parâmetros da pressão sanguínea estimada e os parâmetros extraídos da Eletrocardiografia e da Fotopletismografia. Os segmentos associados a correlações (muito) fortes (coeficiente da correlação de spearman acima dos 70%) foram reunidos para definir o grupo de treino da validação cruzada. Isto permitiu testar a influência, nos modelos construídos, da inclusão de segmentos de biosinais fortemente correlacionados ao invés de biosinais na sua totalidade. Por fim, a influência do processo de calibração implementado, tanto no início da cirurgia (através da computação de um método recursivo dos mínimos quadrados), como durante a mesma (incluindo uma derivação do Tempo de chegada de pulso) foi estudada. Estes modelos foram validados à luz dos protocolos da British Hypertension Society e da Association for the Advancement of Medical Instrumentation, que são considerados os sistemas de medição automatizados *standard* na avaliação da pressão sanguínea. Estes protocolos dependem da distribuição das diferenças entre o valor real e o estimado da pressão sanguínea. O sistema de medição aceite no protocolo da British Hypertension Society requer que pelo menos 50%, 75% e 90% das diferenças mencionadas estejam entre 5, 10 e 15 mmHg, respetivamente, enquanto que a Association for the Advancement of Medical Instrumentation exige que o desvio-padrão e média das diferenças sejam iguais ou inferiores a 8 mmHg e 5 mmHg, respetivamente.

O modelo com melhor desempenho e de acordo com os protocolos implicados não exigiu nem sensores de eletrocardiograma extras nem as calibrações implementadas. Isto corrobora o papel fundamental dos parâmetros da Fotopletismografia incluídos. A estimativa da Pressão do pulso foi a única a satisfazer as exigências de ambos os protocolos, enquanto que as estimativas da Pressão sanguínea diastólica e da Pressão arterial média apenas preencheram as exigidas pela British Hypertension Society. Por fim, a estimativa da Pressão sanguínea sistólica não preencheu nenhum dos requisitos dos protocolos.

De um modo geral, a forte relação entre Pressão sanguínea e Fotopletismografia foi corroborada pelos dados obtidos. Maiores populações heterógenas teriam de ser testadas de modo a poderem ser apresentadas conclusões fiáveis em relação à estimativa contínua e não-invasiva da Pressão sanguínea, baseadas unicamente na Fotopletismografia.

Abstract

This dissertation aimed to study and evaluate the estimation of Blood pressure, on a continuous and non-invasive basis, to be deployed during surgeries, relying only on extracted features from non-invasive modalities (Photoplethysmography and Electrocardiography). From the Photoplethysmography, features were extracted by means of its pulsatile and non-pulsatile components, as well as the corresponding second derivative of the pulsatile component. Namely, the Pulsatile component amplitude, Non-pulsatile component amplitude, Ratio of pulsatile and non-pulsatile amplitudes, Dicrotic notch amplitude, Reflection index, Heart beat interval and the Ratio between amplitudes of the second derivative waveform of Photoplethysmography ("b" and "a" waves). Two different implementations of Pulse arrival time were also computed (according to [65] and [17]) and included in this feature pool which in its turn required the consideration of Electrocardiography in this experimentation. The nine extracted features from these two biosignals had their relationship quantified in terms of the correlation performance with four different Blood pressure features: Systolic blood pressure, Diastolic blood pressure, Pulse pressure and Mean arterial pressure. This analysis highlighted the strong correlations of the Ratio of "b" and "a" waves amplitudes and Pulse arrival time (computed from [17]) with Systolic, Diastolic and Mean arterial pressures for all patients. The spearman correlation coefficients varied between 71% and 90% for the former and between 75% and 91% for the latter feature. In contrast, Heart beat interval only showed negligible correlations with the blood pressure features. Spearman correlation coefficients varied between 4% and 58%.

Furthermore, the Blood Pressure features in investigation were separately estimated from the combination of the nine features previously mentioned through multiple linear regression modelling, for each patient, and confirmed according to a leave-one-out cross validation. Different models were proposed and experimented in order to evaluate the contribution of four major aspects on the estimated Blood pressure features. The influence of the inclusion of Pulse arrival time (and consequent usage of extra electrocardiogram sensors) and Photoplethysmography's non-pulsatile component in the arranged models was taken into account. The biosignals were also segmented and had the spearman correlation coefficient calculated, for each segment,

between the estimated Blood pressure features and the pooled features from Electrocardiography and Photoplethysmography. The segments associated to (very) strong correlations (spearman correlation coefficients above 70%) were assembled to define the training group in the cross validation. This enabled to test the influence, in the built models, of the inclusion of strongly correlated segments of the biosignals, instead of the entire biosignals. At last, the influence of the implemented calibration procedure both in the beginning of the surgery (through the computation of a recursive least squares method) and during the surgery (including a derivation of Pulse arrival time) was studied. These models were validated within British Hypertension Society and Association for the Advancement of Medical Instrumentation protocols, which are considered to be the standards on the evaluation of blood pressure automated measuring systems. These protocols depend on the distribution of the differences between the real and the estimated Blood pressure values. The measuring system to be accepted within the British Hypertension Society protocol requires that at least 50%, 75% and 90% of the mentioned differences to be within 5, 10 and 15 mmHg, respectively, while the Association for the Advancement of Medical Instrumentation demands the standard deviation and the mean of the differences to be lower than or equal to 8 mmHg and 5 mmHg, respectively.

The best performing model according to the implied standard protocols didn't require neither extra electrocardiogram sensors nor the implemented calibrations. This corroborates the key role of the included range of Photoplethysmography features. Pulse pressure estimation was the only to fulfill the two protocols' requirements while Diastolic blood pressure and Mean arterial pressure estimations only met British Hypertension Society recommendations. At last, Systolic blood pressure estimation didn't meet neither British Hypertension Society nor Association for the Advancement of Medical Instrumentation protocols.

Overall, the strong relationship between blood pressure and Photoplethysmography was corroborated for this data. Larger heterogeneous population would have to be tested in order to be presented reliable conclusions on the continuous and non-invasive Blood pressure estimation solely from Photoplethysmography.

.

"In many respects anaesthesia is more an art than a science; most anaesthesiologists believe it is easy to recognize but difficult to define."

Leslie Jameson

Contents

List of acronyms

AAMI Association for the Advancement of Medical Instrumentation

AC PPG pulsatile component

ANB Antinociception-nociception balance

ANI Analgesia/nociception index

ANS Autonomic nervous system

APG second derivative of PPG

BHS British Hypertension Society

BP Blood pressure

BPF BP group of features

CNS Central Nervous system

DBP Diastolic blood pressure

DC PPG non-pulsatile component

DN Dicrotic notch

ECG Electrocardiography

EEG Electroencephalography

EMG Electromyography

GA General anaesthesia

HBI Heart beat interval

HR Heart rate

IQR Interquartile range

LRC Linear regression coefficient

MAP Mean arterial pressure

MLR Multiple linear regression

NoL Multiparameter nociception index

NSCF Number of fluctuations of SC

PAT Pulse arrival time

PP Pulse pressure

PPG Photoplethysmography

PWV Pulse wave velocity

RI Reflection index

RLS Recursive least squares

RMSE Root mean squared error

SBP Systolic Blood pressure

SC Skin conductance

SCA SC algesimeter

SCC Spearman correlation coefficient

SPI Surgical stress index

SSS Surgical stress scales

WTCRC Wavelet transform cardiorespiratory coherence

1

Introduction

1.1. General situation

Surgery was defined as any procedure occurring in the operating room involving the incision, excision, manipulation or suturing of tissue that usually requires regional or general anaesthesia or profound sedation to control pain. Adverse painful events were shown to affect 3% to 16% of all hospitalized patients, when more than half were known to be preventable [1].

"Assuming a 3% perioperative adverse event rate and a 0.5% mortality rate globally, almost seven million surgical patients suffer significant complications each year, one million of whom die during or immediately after surgery" [1]

Anaesthesia experts reviewed other industries known as high-reliability organizations (aviation, nuclear power, for instance) and to meet the same demanding level, acknowledged the persistence of human error in the anaesthesia depth assessment [1]. This propelled the improvement of anaesthesia depth understanding (both analgesic and hypnotic components) in terms of physiological dynamics.

Through the autonomic nervous system (ANS) a response is delivered when some noxious stimulus is inflicted. This stimulus is detected by peripheral sensory neurons, known as nociceptors. Then, it is encoded and processed, in a process known as nociception [2].

The induction of general anaesthesia (GA) prevents nociceptive events to trigger an ANS response. The GA requires a continuous control over the analgesics (most commonly opioids) and hypnotic drugs administration, throughout the surgery. These substances are responsible for the decrease of the ANS reactivity to the nociceptive stress (through the blockage of the sensory neurons activity) and for the induction of a sleeping state, respectively. Altogether, this reaction is known as antinociception. [1] expressed the complexity and the consequent implications that an improper monitorization of anaesthesia might have, which can even lead to a paradoxical hyperalgesia situation.

Nevertheless, none of the administrated drugs has full potential to cover all the needs by itself and protect the patients from the undesirable cardiovascular

(bradycardia, hypotension) or respiratory suppression (and consecutively, hypoxia) events [1]. This means that a wise combination of anaesthetics is required, which depends not only on the specific surgical characteristics, but also on the properties of each drug wherein it needs to be considered medication reactions and interactions.

From the lack of physical response to stimulation, it doesn't follow that the homeostasis is in control. This obliges the anaesthetist to follow the evolution of basic hemodynamic parameters controlled by ANS such as Heart Rate (HR), Systolic Blood Pressure (SBP) and Pulse Oximetry [3]. For the time being, in order to complement the traditional monitoring, it might be integrated some available regulatory index [4]. So far, no index has been yet standardized given the inexistence of a ''gold standard'' objective score that suits as an intra-operative nociception reference for further reliable validation.

On the one hand, the permanent perioperative reactivity (including reflex responses to noxious stimulation, but also somatic, autonomic and endocrine reflexes) or post-operative side-effects (related with recovery) exhibits the emergent need to create a holistic feedback system which is able to quantify all these events, in terms of their implications towards the patient's homeostasis.

On the other hand, it is required a standard real measurement on the nociceptive stress during anaesthesia or, in other words, a certified reference to validate the final predictions on the patient's homeostasis, here denominated as surgical stress scale (SSS).

So, in order to further explore this subject, it was initiated a dissertation, involving both Coimbra's university and Patient Care & Measurements Philips Research department, in Eindhoven.

1.2. Motivation

Currently, the most basic approach used in the regulation of the patients' homeostasis is based on Pulse rate and Blood pressure measurements monitoring. However, the refinement of this reference has been attempted. The very first SSS didn't fully reflect the nociception scope. For instance, [5] elaborated an SSS which was based

on comparison to clinical scores for adequacy of the hypnotic component of anaesthesia, such as Observer assessment of awareness and sedation score (OAA/S score) [6,7]. Unfortunately, these scores no longer apply to anaesthesias given the changes that the surgeries agendas suffered, where the new introduced drugs led to the patient's response loss of verbal and physical stimuli [8].

More recently, this SSS concept was further developed by combining nociceptive stimulus to the analgesic drug effects in an antinociception-nociception balance (ANB). For instance, both [8] and [9], created an SSS which are based on linearly combined stimulus intensity (nociception) and analgesic concentration (anti-nociception) scales. On the one hand, the stimulus level was based on experienced anaesthesiologists expertise and on the other hand the analgesic level depended on the effect-site concentration of opioids.

Despite none of the existing SSS is yet fully explanatory, various indexes have been implemented and tested in particular conditions that depict as close as possible the surgical events. These indexes aim to regulate homeostasis based on the behaviour of certain vital signs or biosignals, such as Photoplethismography (PPG) and Electrocardiography (ECG), and their corresponding features while fulfilling surgical's requirements (e.g. ease to acquire, constrain of the medical procedure). Although there are some promising results, they are always specific to the physiological characteristics of the tested population and tend to fail when applied to a more heterogeneous population. Another aspect that's holding back further progress is the currently attained idea of nociception. It needs to move from a merely binary process to a phenomenon with intermediate levels [5], where various clinically relevant end-points (e.g. loss of consciousness, recovery of consciousness, postoperative recall) are likely to occur at different thresholds [10]. These drawbacks are very difficult to address in practice though, given the medical expertise it requires.

However, not all biosignals have been fully inspected so far. The absence of Blood Pressure (BP) from the existing solutions is notorious. Even though it reflects the cardiovascular status and consequent patient's awareness [11], a reliable continuous and non-invasive measurement of BP hasn't been yet provided. For this end, and inspired by a relevant waveform similarity [12], PPG features were found to have some degree of correlation with BP features which could contribute for BP estimation. For

instance, PPG pulsatile component (AC) and BP share a strong relationship with the same cardiovascular physiological manifestations [13]. Also, the second derivative of the PPG waveforms (APG) are known to be an indicator of the acceleration of the blood in the finger. It reflects some characteristics such as arterial stiffness to which BP measurements are dependent on [14].

Within Philips research group of 'Patient Care and Measurements' department, Dr. Jens Muehlsteff reported some events where the variations in BP weren't corresponded with the physiologically expected response from PPG. For instance, figure 1 depicts one situation where an increasing Mean arterial pressure (MAP) is accompanied by a simultaneous unexpected increase in the AC amplitude (AC_A) while the expected relationship would be the opposite [15]. The implications of this counter intuitive scenario are that these features' measurements, being both markers of the vascular system homeostasis, are complementary. So, they are not able to separately provide the sufficient information to express the vascular system activity. In other words, the fact that both these signals describe the same physiological structures but sometimes present characteristics that behave differently means that there are some physiological factors which influence one of the signals but not the other. Therefore, the introduction of BP in a surgical scenario becomes decisive.

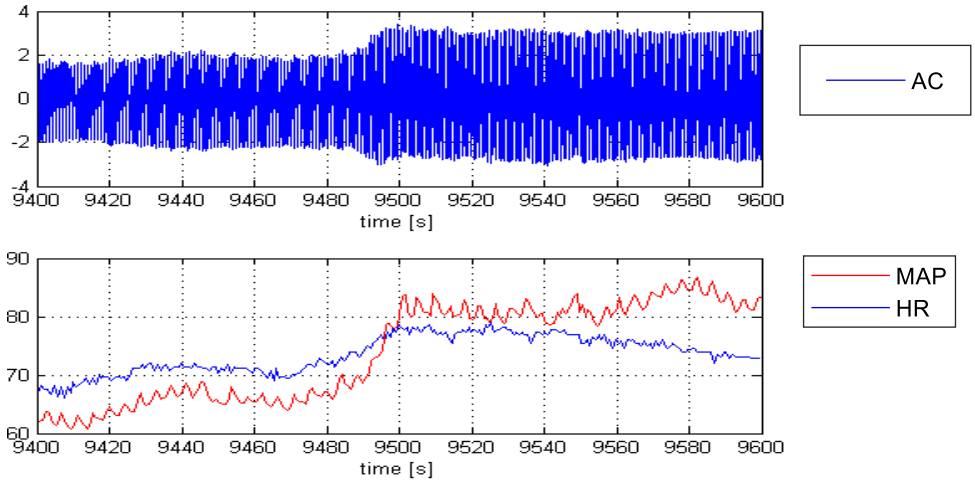

Figure 1: Reported increase in AC_A (upper panel) accompanied by an unexpected increase in MAP. HR and MAP were used as references for the depicted observations. Adapted from Dr.Jens Muehlsteff previous reports.

This corroborates the hypothesis that BP continuous readings could become useful to the issued nociception problem. This premise has already been taken into account in some previous studies. [8] showed that the introduction of non-continuous BP helped to improve the proposed Surgical stress index (SPI) correlation with ANB through the reduction of the residual error. Also, the possible contribution of continuous and non-invasive BP measurements, acquired from a single finger probe, was considered in the multiparameter nociception index (NoL) [9]. However, its validation hasn't been tested yet given that the current technology does not allow reliable BP measurements from a finger probe.

1.3. Goals

So, motivated by these facts, an inspection towards the validation of the correlation between BP and PPG features was proposed in order to include an easily acquired BP continuous estimation, using PPG properties, in the evaluation of ANB. The assumption that the reported inconsistencies by Dr. Jens Muehlsteff might have had disturbed the estimations were also taken into account. In a second stage, the ECG was also considered in order to inspect the usefulness of Pulse arrival time (PAT) in this estimation. Over the past recent years, this feature has been highly addressed with success regarding the estimation of SBP. Therefore, it is a good point of comparison with any other feature.

The fact that PPG and ECG are already being collected during surgeries gives room to the exploitation of their potential, easing up also the final index deployment in the real situation and its acceptance in the medical community. The integration of these biosignals in a reliable continuous and non-invasive BP estimation solution would be a great asset in the improvement of some already existing index or in the creation of a new one. Nevertheless, its continuous and non-invasive measurements would already be clinically rewarding instead of being either dependent to the typically available 5 min intervals of BP measurements which hardly provide insights in the short-term responses (to noxious stimuli) or any existing invasive solution which is harmful for the patient.

The main disruptive contribution in this dissertation is the presence of the non-pulsatile (DC) measurements which is thought to have a vast potential to be explored in terms of its correlation with BP features, namely the scarcely reviewed Pulsatile and Non-pulsatile components amplitudes' ratio ($\frac{AC_A}{DC_A}$). PAT is also highlighted given the large number of associated reviews in this subject which use it to reach a BP measurement.

Overall, BP had SBP, Diastolic blood pressure (DBP), Pulse pressure (PP) and MAP inferred based on a multiple linear regression (MLR) model, combining PAT, AC_A, DC amplitude (DC_A), $\frac{AC_A}{DC_A}$, Dicrotic notch amplitude (DN), "b" and "a" waves amplitudes' ratio ($\frac{B}{A}$), Reflection index (RI) and Heart beat interval (HBI).

1.4. Structure

In terms of structure, at first all the implied biosignals and indexes in the ANB solving as well as the strongly correlated features between PPG and BP will be reviewed in the state of the art.

This will be followed by the data & methods chapter where patients' information is given, and SPI and ANI are reviewed, based on the implementation which was carried out in the initial phase of this dissertation. It is also explained which features from each biosignal were used and all the processing they went through. The final consequent analysis of the relationship between both PPG and ECG features with BP features is followed by the final BP assessment.

After this, all the results are presented and interpreted in the results and discussion chapter. In the conclusion, it is suggested some of the future work that could to be done.

.

2

State of the art

2.1. Physiological background

Currently, there is an effective struggle in what concerns to the reliable and continuous monitoring of perioperative hemodynamic instability by anaesthetists. In its turn, this instability is associated with adverse cardiovascular events which have been statistically shown to contribute to postoperative morbidity. The management of BP and HR has been standardized as the key factor for maintenance of surgical setting. Nevertheless, it lacks a precise control of the depth of anaesthesia, considering the interindividual variability which is observed in response to different stimuli and administered drugs [15,10]. In a broader scale, it is required a system which measures the effective anaesthetics dosage according to the nociceptive stress.

First, in order to proceed with the analysis, it is necessary to clarify the difference between nociception and pain, which can be done by analysing the predominantly involved neuroanatomical structures from Figure 2. Nociception refers to the stimulation of any of the central nervous system (CNS) structures (through which peripheral stimuli is transmitted) that precede cortex, whereas pain can only be experienced when nociception is translated in the cortex.

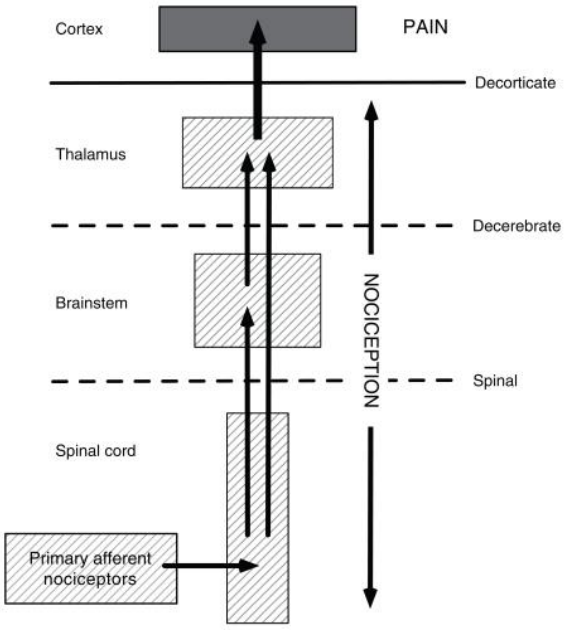

Figure 2: Key anatomic structures of the CNS in the nociception and pain perception. Source: [7]

The management of nociception avoids the occurrence of any main changes in the pain pathways, which can lead to cronic states, so that patients under anaesthesia can stay out of danger [5].

Nociception is evoked when the primary afferent nociceptors detect potentially harmful stimuli such as pressure or temperature extreme variations. In its turn, nociceptors can be characterized by their capacity to tolerate that same variations. Physiologically, this characterization depends on two references: pain threshold and pain tolerance. The former outlines when the body first perceives stimulae as harmful and it is surpassed by the latter which establishes the maximum level of pain that a person is able to tolerate. Eventhough the relationship between these two references is easy to understand, there are various types of specialized receptors which are activated through different sensory modalities. Also, the way the sensory information is sent to the brain depends on the frequency of the action potentials and the number of activated receptors. Ultimately, the intensity discrimination of the arising stimulus results from a non-linear perceiving process by the brain [17].

Furthermore, the resulting stress response is characterized by an activation of the ANS. ANS is responsible for the control of breathing, cardiac activity, vasomotor activity and certain reflexes such as coughing, sneezing, swallowing and vomiting. Therefore, the manifestation of nociceptive stress can be noticed through variations in physical signs, heart beats, vasomotor tone, stroke volume, blood pressure, respiration rate, body temperature [18]. In order to avoid the patient from awakening in a surgical scenario, it is required to inhibit the stress response. In other words, the aforementioned pain tolerance can’t be exceeded.

For that end, GA is induced through hypnotics and analgesic agents which induce an altered state of consciousness and abolish the nociceptive responses, respectively, while operating in the cortex and thalamic areas of the brain. They must be carefully used according to both patients’ needs and the other anaesthetic agents which they are being combined with.

At this point, the knowledge of the minimal effective doses of the anaesthetics to be administrated throughout the operation (accordingly to the patient’s homeostasis) is still missing. An underdosing can lead on to intraoperative awareness (whose causing

events might even be recalled afterwards) whereas an overdosage might lead to delayed recovery. The exact mechanism by which these drugs lead to an anesthetic state is not yet fully understood. Some of the administered drugs during the perioperative period have a cardiovascular modulating potential and may act through different mechanisms (activation or depression) which contribute to the mystification of the entire process [7]. Therefore, the measurement of the depth of anaesthesia is still a complex concern for the anaesthetists.

The first generally accepted classification system to detect states of inadequate analgesia was Guedel Classification. It depended on the eyelash reflex, respiration, eyeball movements, pupillary size, and muscular movements among others physical signs. Similarly, Visual analog scales provide a 0-100 pain scale which is generally completed by patients themselves or sometimes used to elicit opinions from health professionals, at every specific interval. With the introduction of muscular relaxants and the combination of multiple drugs, these systems became obsolete [4], given to the physical signs absence which arose from the patient's non-responsiveness.

To augment their expertise regarding the analgesia suitability, clinicians started to continuously monitor mainly breathing and circulation. To do so, they inspect fluctuations on HR and BP measurements which are displayed on any current monitoring device [1,10]. However, the subjectivity that relies upon any clinical decision, while interpreting the latter specified information, is always associated to some percentage human error. A complementary quantitative solution towards the nociceptive stress awareness is demanded.

2.2. Biosignals

The ANS activity concerning nociception and GA drugs effects may be inspected through the Electroencephalography (EEG). It supplies the clinician with a direct measurement of the brain's electrical functioning. In its turn, in order to read the useful information provided by EEG, features have been extracted in the frequency or time domain. However, in this specific situation, EEG complex analysis, poor signal quality and patient discomfort undermine its interpretation in an operating room.

Meanwhile, the ANS manifestation can be depicted through other available biosignals which bring together many more favourable characteristics. Electromyography (EMG) enables to regulate nociceptive stress from the variations in muscular electrical activity to predict patients' movements when the induced anaesthesia is inadequate. Then, PPG provides the monitoring of the peripheral vascular system where the standard waveform may be regarded in two phases. The first phase concerns the systole while the second phase concerns the diastole and waves' reflections from the periphery. Furthermore, ECG is intimately associated with the heart functioning and enables the extraction of HR (standard reference for the clinician). When GA is well stabilized, the RR series (extracted from ECG) is only modulated by Respiratory Sinus Arrhythmia which allows the appearance of a ventilatory pattern at regular intervals. When stimulated, this pattern changes. Also, Skin conductance (SC) has been addressed given that it is associated with the skin sensors' activity. Skin resistance is known to vary with the state of sweat glands in the skin. All these options are described in table 1 in terms of their useful features and consecutive perceivable physiological activity and characteristics which are known to be manifestations of nociceptive stress.

All the considered biosignals in table 1 relate to the ANS misbalance through the respective physiological characteristics they report about. Also, the listed features are more useful when combined, to form indexes, which allow a better insight on the ANS activity. However, not all biosignals have been concerned in the existent indexes' implementations due to some limitations. For instance, BP is known to be desirable either in surgical procedures or intensive care units, however it still lacks a reliable non-invasive continuous measurement of BP [19,20,21]. Also, the implementation of a worldwide standardized ANB monitoring solution needs to consider some human and equipment restraints.

2.3. Nociception indexes

Some of the most evaluated indexes was set up together and characterized: Wavelet transform cardiorespiratory coherence (WTCRC), Bispectral index (BIS), CARDEAN, SPI, ANI, SC algesimeter (SCA) and NoL.

Table 1: List of Biosignals described accordingly to their mainly reported features and the corresponding physiological characteristics and activity they have been associated to

Biosignal	Physiological characteristics/activity	Features
PPG	Stroke volume, systemic vascular resistance and compliance [22,23]	AC_A
	Average blood volume [23]	DC_A
	Systemic vascular resistance and compliance, wave reflection [14]	RI
	Arterial stiffness and systemic vascular resistance [14]	Arterial stiffness index (SI)
	Vasomotor tone [22]	DN
	Systemic vascular resistance [14]	Pulse width
	Heart beating activity [14]	HBI
	Arterial stiffness [14,24]	$\frac{B}{A}$
	Pulmonary activity [25]	Respiration rate
ECG	Heart beating activity, cardiac output [7,18]	HR
	Respiratory sinus arrhythmia [10]	HRV
EMG	Number of recruited motor unities [26]	Root mean square
	Changes on the motor unities which are being recruited [26]	Power spectral density
EEG	Energy shift from higher to lower frequencies in EEG activity [7]	(Alpha waves ratio) - (Beta waves ratio)
	Thalamocortical pathway activity [7]	Bispectral analysis
	Percentage of isoelectric EEG activity [7]	Burst suppression ratio
BP	Cardiac output, systemic vascular compliance and resistance [27]	SBP
	Vascular tone [27]	DBP
	Ventricular ejection volume and rate, systemic vascular compliance [27]	PP
	Cardiac output, systemic vascular resistance [27]	MAP
SC	Electrical conductance variation (promoted by sweat production) [10,28]	Number of fluctuations of SC (NSCF) (e.g. peaks/sec)
	Basal level of electrical conductance [29]	SC level
Respiration	Respiratory distress, cardiac arrest [30]	Respiratory rate

Firstly, the computation complexity of each index influences its real-time monitoring performance, by delaying the estimation process. For instance, EEG holds complex waveforms which require the exploration of combined computationally heavy features in order to assess the different kinds of drug interaction [7]. Although this information hasn't been provided for all the considered indexes, it is assumed that the real-time feature is assured at least for those indexes which are already commercially available.

Then, it is also concerned the drawbacks of the implementation settings of the monitoring system and whether the used sensors are already clinically available in a standard anaesthesia monitoring. For instance, SPI only requires a PPG finger probe whose design is a perfect fit given the size, sensitivity, reliability and reproducibility requirements [14], whereas WTCRC is dependent on both ECG electrodes and capnometer which are uncomfortable for the patient [31]. Although both of these biosignals are already measured in a typical surgery, other indexes require specific sensors which are not available in every operating room (e.g. CARDEAN). This has implications in a major scale when the implementation and standardization of a new surgical assessment tool is attempted, given the economic feasibility the solution demands. Therefore, if the indexes involve biosignals which are already clinically available in a standard anaesthesia monitoring, it is preferable. Physiological artifact, reported relationship breaches with ANB and anaesthetics are also comprehended for the current biosignals, in table 2.

From a clinical point of view, an ideal index immediately detects any ANB misbalance, it is easily installed and interpreted, assisting the anaesthesiologists with a ranged scale, and its implementation makes no harm to the patients (e.g. non-invasively measured). Some technologies are already commercially available such as SPI, SCA, ANI, BIS, others are still under development such as CARDEAN, WTCRC, NoL [32]. The combination of multiple nociception related parameters, which is thought to have more ability to read the synergistic physiological functioning [33], demonstrated stronger relationships with ANB when compared with any single-parameter based approach [8,9]. Even though all these tools have proven ability to evaluate the ANB, none has been accepted as the gold standard yet. The permanence of some limitations

such as the limited number of highly homogeneous patients in validation and the limited drug combination depreciates these indexes against the standardized control of HR and BP (and the human errors it brings) [33,7].

Currently, the monitoring tools are mainly used on those situations where the limitation of sedation is beneficial to the patient. According to the clinical context, whether it is important to limit the opioid administration, the postoperative pain, the patient movements or hemodynamic reactivity, the anaesthesiologist chooses one of the available indexes to complement and support his decisions [32]. Otherwise, there is no need to invest in extra equipment or training (e.g. nurses don't handle this equipment on a general basis) since no significant improvement for the anaesthesia adequacy is visible [7,34].

2.4. BP estimation

From the previously reviewed indexes, all of them involve non-invasive techniques. This helps to expose the patients to a minor infection risk and other adverse effects such as distal ischemia, bleeding, which are associated to increased morbidity and costs [35,36]. From table 1, the only biosignal which doesn't meet these measurement requirements is BP. Reliable continuous BP measurements are only available in an invasive way. For instance, arterial tonometry measures BP on a continuous and non-invasive basis, however it is dependent on the optimal placement of the measuring device on the artery. Therefore, in order to enhance the current ANB assessment, it was proposed to include a BP estimation in the nociception assessment problem.

Numerous attempts have been made to estimate BP from derived features of other biosignals in different experimental settings, though with some associated drawbacks.

Table 2: List of the most reported and tested nociception evaluating indexes in terms of their features and corresponding computational complexity, their main limitations (implementation settings, physiological artifacts, reported relationship breaches with ANB and anaesthetics) and the type of sensors and whether they are available in a typical operating room

INDEX	Features (**computational complexity**)	Limitations	Sensors (**available in typical surgery**)
SPI	HBI, DC_A	• Physiological artifact: vasoconstriction, hypovolemia or hypothermia and a history of chronic elevated blood pressure [37] • Unable to differentiate stimulus intensities [5] • Inter-individual variability [5] • Requires initial calibration through specific procedure [8]	PPG finger clip sensor (**YES**)
ANI	HRV high frequencies **(Prolonged calculation time period [3])**	• Wearing the ECG electrodes for quite longer duration lead to patient discomfort [31] • Physiological artifact: arrhythmia, apnea or low respiratory frequency [37] • Premature ventricular and atrial contraction are misunderstood with noxious stimuli • Validated threshold on hemodynamic reactivity [38]	3 electrodes (for ECG lead) (**YES**)
BIS	Burst suppression Ratio (time parameter), Relative beta Ratio (frequency parameter) and SynchFastSlow (higher order statistical parameters) **(computationally heavy parameters)**	• Poor contact with electrode [7] • Dependent on manufacturer's recommendations; • Corrupted by routine intraoperative events (activation of electromagnetic devices, administration of depolarizing muscle relaxants) [10] • Physiological artifact: hypoxia, hypotension, cerebral ischaemia or hypoperfusion, muscular activity [7,10] • Insensitive to commonly used anesthetics (ketamine) [37] • Insensitive to analgesic component [17] • Dysfunctional behaviour when the patient's EEG activity is approximately null • Lacks an underlying physiological model on the brain functioning and awareness generation [39] • No absolute threshold has been found that could be predictive of amnesia or recall	Head covered by mob cap of electrodes (**ALMOST NEVER**)
SCA	NSCF **(Computationally light parameters [5])**	• Stretching of wires [5] • Electrode dislocation [5] • Environmental temperature [5] • Physiological artifact: coughing, deep respiratory movements, sneezes, excess sweating [5,28,40]; • Insensitive to commonly used anaesthetics (atropine) [10] • Small correlation with opioids [5]	3 self-adhesive electrodes in palmar or plantar skin (**ALMOST NEVER**)

Table 2 (continuation): List of the most reported and tested nociception evaluating indexes in terms of their features and corresponding computational complexity, their main limitations (implementation settings, physiological artifacts, reported relationship breaches with ANB and anaesthetics) and the type of sensors and whether they are available in a typical operating room.

INDEX	Features (**computational complexity**)	Limitations	Sensors (**available in typical surgery**)
CARDEAN	SBP, HRV	• Electrodes are uncomfortable (if worn for a long time) [31] • Finapres BP sensor requires intervaled calibration [33] • movements blunted with sympathetic bursts [41] • designed for movement prediction on non-paralyzed patients • Reports only the hypertension-tachycardia balance [41]	Non-invasive continuous BP sensor (Finapres medical systems) and 3 electrodes (for ECG lead) (**ALMOST NEVER**)
NoL	HR, HRV, PPGA, SC level, NSCF and SC derivatives	• The effects of hypnotics on NoL need to be investigated [9]	PPG finger clip sensor and SC electrodes regrouped in the finger sensor PMD-100TM (Medasense Biometrics) (**ALMOST NEVER**)
WTCRC	HR and respiration CO_2 waveform **(Computationally inefficient with real time delay [32])**	• Electrodes are uncomfortable (if worn for a long time) [31] • Capnometer is uncomfortable and interferes with normal breathing • Affected by arrhythmia or apnea [37] • Imprecise [32]	3 electrodes (for ECG lead) and capnometer (**YES**)

The relationship between vessels' volume and pressure expresses itself through PPG and BP approximated waveforms [12]. This similarity brought into attention a possible solution for the noninvasive beat-to-beat measurement of BP which hasn't been reached yet because of absent standardized equipment and understanding of the underlying physiology of the PPG [15]. [21] devised a wearable device based on two PPG sensors which estimates BP from pulse wave velocity (PWV) in peripheral arteries. This method is based upon the high correlation between PWV and BP. However, the concerned relationship requires initial calibration. [42] proposed an estimation of BP from raw PPG signals, employing a deep learning technique. However, the model was computationally intensive and tested in patients with a stable BP recording (absence of abrupt BP variations which are the most difficult to monitor).

The derivatives of PPG were also exploited against BP derived features. The APG waveform offers more information than the 1st derivative and so it has been more oftenly used [14]. [43] concluded that the measurement of SBP is improved when the data is divided in several classes, according to their APG derived "b" and "d" waves, and evaluated separately. Subsequently, these features were considered to be related with cardiovascular peculiarities. Furthermore, APG derived features are also used as ratios. [24] studied the influence that age and SBP exert on $\frac{B}{A}$, which in its turn correlated negatively with both. Despite both studies focused on people with specific characteristics (60-year-old subjects and above [43] and hypertensive patients [24]), the results for this kind of methodology were promising.

Other works have presented alternative solutions towards the BP assessment which require the usage of multiple biosignals. For instance, the variations in BP have been shown to be correlated with the PAT.

[19] estimated SBP from PAT during a cardiovascular surgery but it required an intermittent calibration obtained with the auscultatory method. Furthermore, [44] reported a method for estimation of DBP and SBP through PAT supported by two confounding factors: HR and arterial stiffness. This method was evaluated in surgical and unconstrained scenarios where the confounding factors were proved to improve the PAT based BP assessment. However, a complex initial calibration was required.

[12] estimated SBP from ECG and PPG based features during a 40 minutes exercise where a relevant role was attributed to PAT which improved the final results. However, the reference was not invasively measured (which is not as accurate), the controlled conditions of the tests suppressed typical motion artefacts and a time consuming initial calibration was also required. [45] depicted the monitoring of BP from PAT in unconstrained scenarios. The significant effects that posture change has on PAT measurements didn't allow a reliable BP inference where the importance to access context is emphasized (e.g. the subject's posture), given the unsupervised monitoring. [46] characterized the syncope reflex mechanisms and BP changes from the analysis of non-invasive modalities (ECG, PPG and impedance cardiogram). Bradycardia and hypotension were observed to result in syncope. The significant increases of PAT, Pulse transit time and Stiffness index, preceding these syncope occurrences as well, suggested the suitability of these features as surrogates for SBP.

2.5. Proposed research

According to the literature, two groups of features were proposed: the ECG and PPG group of features (PEF) and the BP group of features (BPF).

On the one hand, features from PPG biosignals were pooled. The waveform and reflected physiological characteristics that PPG has in common with BP makes it the most adequate option for this task. The less reviewed ratio $\frac{\mathrm{AC_A}}{\mathrm{DC_A}}$ was added to the set, in order to explore its potential. The large quantity of projects on the BP estimation from PAT, based on their strong relationship, led to the introduction of PAT in the range of features as well. This required the involvement of ECG. In general, none of these features requires complex calculations. On the other hand, it was extracted MAP, PP, SBP and DBP from the BP.

The 3 implied biosignals were carefully chosen not only because they reflect ANS activity but most importantly because ECG and PPG continuous non-invasive measurements are available in every operating room. The latter eases up the implementation of the BP estimation method in the surgical scenario. The implicit features are summarized in the next chapter.

The assessment consisted of performing MLR through computation of the linear least-squares estimates of the regression coefficients. It is a straightforward and simple parameter estimator. More advanced models could be used (such as random forest, linear ridge or support vector regression) which deal better with the non-linear complexity of the ANS but the results were expected to be very similar, though. The concerned small sample size usually leads to overfitting, independently of the used regression techniques [9,12]. Also, this experimentation was not the main target of this dissertation

3

Datasets and Methods

3.1. Datasets

The dissertation analysed the data from a total of 3 individuals (patient 1,3 and 5) which was made available by Philips. For each subject, it was continuously collected non-invasive ECG and infrared PPG and invasive BP measurements (figure 3), during surgical scenarios, in the Tilburg hospital of Eindhoven. The sampling rates of ECG, PPG and BP was 250 Hz, 125 Hz and 125 Hz respectively. Data's annotations by the clinicians, such as intubation and incision events, are very rare and not fully synchronized (until 1 min delay). If the noxious stimuli are not precisely registered in a time scale, their subjective identification is of low value. Instead, the entire procedure was divided in the following stages: firstly, it was induced anaesthesia. This anesthetic state was maintained throughout the entire surgery with ventilation. It had to pass some time from the beginning of ventilation until the surgical period started. The analysis that follows considered only the surgical period which was of 2h24min, 3h1min and 3h17min for patient 1, 3 and 5, respectively. Signal processing and statistical analysis were carried out using MatLab.

3.2. Methods

This dissertation started with the ambition to infer BP variations in a continuous and non-invasive way, using the PPG, to offer beneficial information for the nociception evaluation. Since it is difficult to precisely quantify hemodynamic reactivity in terms of BP variations, and any attempt to define such cases would be always subjective, the main goal became the inference of BP in a continuous and non-invasive way.

3.2.1. SPI and ANI computation

Firstly, both ANI and SPI were computed according to the publically provided information on these two algorithms, so that a more proper knowledge of two of the best performing and more validated nociception indexes could be acquired and interpreted. On the one hand, ANI depends on HRV which can be measured from the RR series computation. It considers moving windows of 64 seconds, where each RR

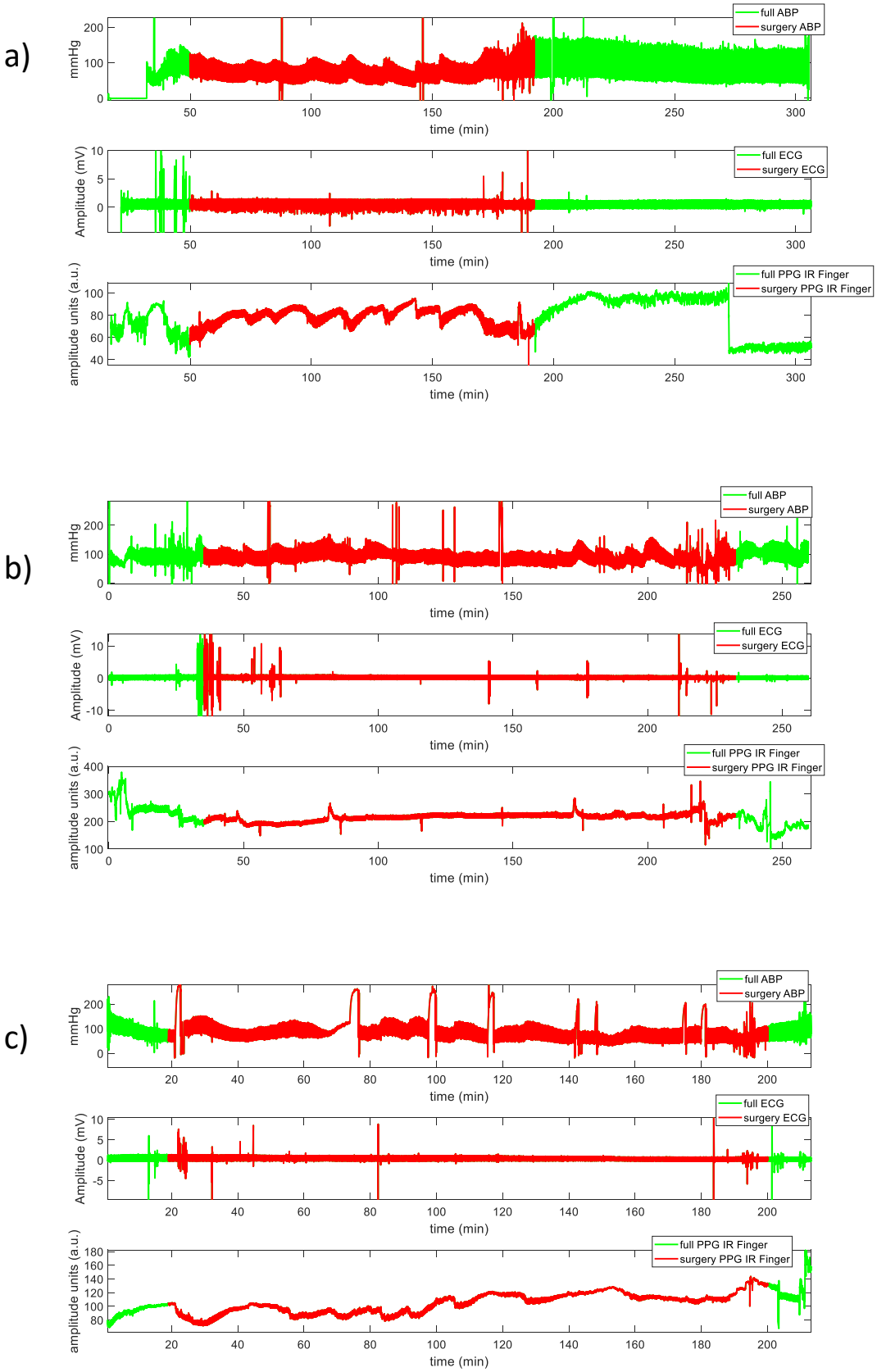

Figure 3: Representation of the entire signals (PPG, BP and ECG), with discriminated surgical period, for patient 1,3 and 5 in (a), (b) and (c) respectively.

sample is normalized within that window (equation 1). Real time calculation provides ANI values every 4 seconds.

$$RR_i' = \frac{RR_i}{S} \quad (1)$$

, where $S = \frac{1}{N}\sum_{i=1}^{N}(RR_i)$; RR_i= RR samples values (after being resampled and mean centered); N= number of samples in the window

After the normalization, the RR series is band pass filtered between 0.15 and 0.5 Hz (high frequencies). From the resulting series, it is drawn a lower and an upper envelope between minimum and maximum detected points, respectively, so that the area between these envelopes could be measured in 4 sub-windows of 16 seconds each (figure 4). The sub-window with the smallest area allows to derive ANI (equation 2). More computation details in [47].

$$ANI = \frac{5.1 * AUC_{min} + 1.2}{12.8} * 100 \quad (2)$$

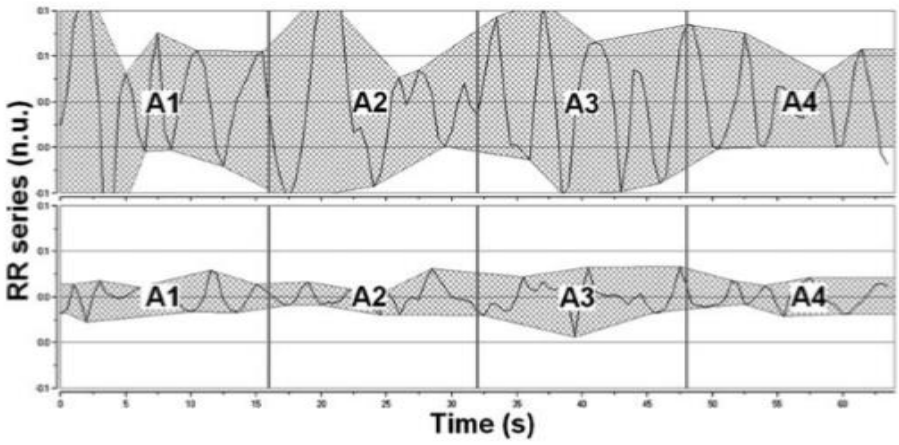

Figure 4: Measurement of RR series in a 64 seconds window during general anaesthesia concerning an adequate analgesia (upper panel) and in the case of surgical stimulus (lower panel). Source: [48]

On the other hand, SPI depends on two derived features from PPG: PPG amplitude and Heart beat interval. These two features were normalized according to a histogram transformation which returns the percentage of the measured values smaller than or equal to the transformed value (0% to 100% scale). Initially, this transformation implies

the apriori knowledge of the distribution of each feature (PPGA and HBI) in a large training group. With the increasing amount of collected data from the patient, this group distribution is combined with the individual distribution of the features (from the patient under anaesthesia). The weight of the individual transformation increases with the amount of collected data (figure 5). After 5 min, the weight of the individual distribution is fixed to 70% (which corresponds to a weight of 30% for the group distribution within the combination). The combination of the distributions is modelled as being normal. Also, while its standard deviation is fixed, the mean corresponds to the mean of the collected data.

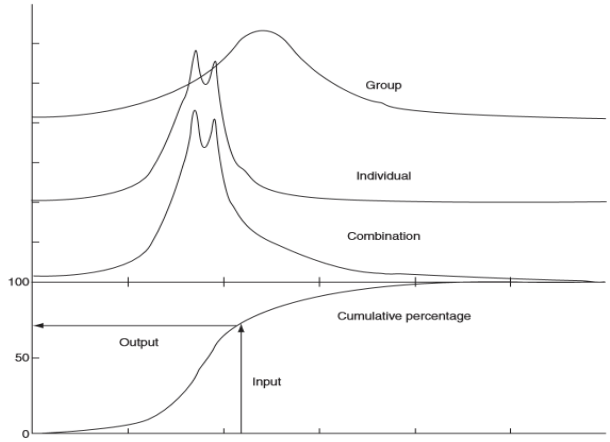

Figure 5: Example with the representation of the group distribution, individual distribution and the resulting combination of these two. The lower panel depicts the transformation function (cumulative distribution). xx-axis: input value of the parameters. Source: [8]

After this normalization procedure, each parameter is combined (equation 3). More computation details in [8].

$$\text{SSI} = 100 - (0.7*PPGA_{norm} + 0.3*HBI_{norm}) \quad (3)$$

The goal of this stage was solely to evaluate qualitatively the behaviour of these indexes and depict any good figures concerning their relationship with the BP. These tests were made with the publicly available database MIMIC II.

This stage was followed by the inclusion of a continuous and non-invasive estimation of BP in the ANB assessment, as the figure 6 depicts with a blocks diagram. The aforementioned multi-step methodology in figure 6 can then be described:

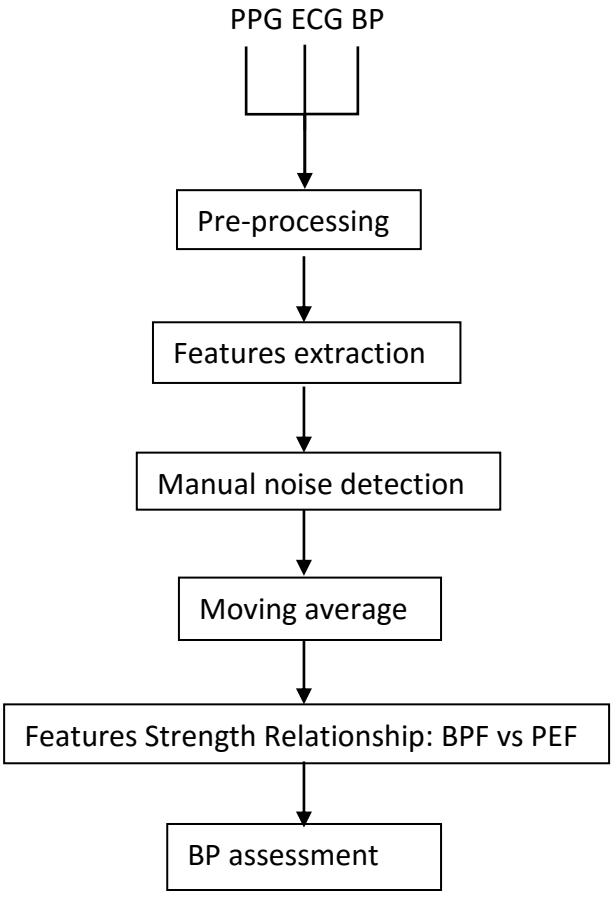

Figure 6: Proposed BP assessment approach

3.2.2. Pre-processing

Firstly, a pre-processing in PPG is required, in order to separate the baseline drift, which corresponds to the DC of the biosignal, from the remaining pulsatile component (AC). DC energy is said to be located within 0.1 Hz and 0.5 Hz range in the frequency domain [49]. So, in order to remove it, the raw biosignal was high pass filtered with a cut-off frequency of 0.5 Hz by a digital infinite impulse response filter with an order of 5.

After the DC removal, an yy-axis flip of the biosignal was done in order to consider it as a representation of blood volume change instead of collected light by the sensor. The obtained component corresponds to AC, from which all the PPG features will be extracted (except for DC_A).

The BP was low pass filtered with cut-off frequency at 10 Hz by a digital infinite impulse response filter with an order of 5, so that high frequency noises could be removed.

3.2.3. Features extraction

Considering all the present concerns in the table 1 (from the state of the art), different BP and PPG features were described from a physiological point of view. Given the similarities in terms of the reflected ANS functions, on the one hand SBP, DBP, PP (equation 5) and MAP (equation 4) were extracted from BP (BPF) and on the other hand, HBI, AC_A (amplitude "x" in figure 7.a), DC_A, $\frac{B}{A}$, RI (equation 6) and DN were extracted from PPG. While HBI, DC_A and $\frac{B}{A}$ are negatively correlated with BP; RI, DN and AC_A are expected to be positively correlated with BP. From chapter 2.4., PAT was also highlighted given the numerous reviews which have emphasized its relationship with BP features whose underlying mechanisms define that BP increases as PAT decreases. Also, $\frac{AC_A}{DC_A}$ was proposed in order to explore its response in such inconsistent situations as those reported by Dr. Jens Muehlsteff. It was expected a positive correlation between BP and $\frac{AC_A}{DC_A}$. Therefore, PEF assembled HBI, AC_A, DC_A, $\frac{B}{A}$, RI, DN, $\frac{AC_A}{DC_A}$, and PAT. Only the last variant obliged the inclusion of ECG information.

$$MAP = \frac{SBP + 2 * DBP}{3} \quad (4)$$

$$PP = SBP - DBP \quad (5)$$

$$RI = \frac{y}{x} \quad (6)$$

, where y and x are represented in figure 7.a)

Exclusively, PAT was implemented in two different ways:

- PAT_1: computed according to [46] which considers the time interval between the apex of the R wave of ECG and 20% of the AC_A (during the upstroke of the PPG pulse), in the same heart beat;

- PAT_2: computed according to [19], the same calculation of PAT_1 was regarded which in its turn was used to achieve an SBP estimation (SBP_e). This estimation is showed in equation 7, where SBP_b is the result of a linear interpolation from the discrete measured points at a regular calibration interval of 5 minutes, ΔT is the change in PAT_1, φ is a fixed coefficient equal to 0.016, T_b is the PAT corresponding to the SBP_b. PAT_2 is considered to be equal to SBP_e.

$$SBP_e = SBP_b - \frac{2}{\varphi * T_b} * \Delta T \quad (7)$$

Contrarily to the PAT definition in the state of the art, the onset of PPG was not considered. Its precise location is difficult to identify given the wideness of the valley it is in. The alternative method was to use the mentioned percentage amplitude which has a minor error associated to the detection of its location in every event (similar to $PAT_{derivative}$ in figure 7.c . Meanwhile the R peak in ECG was detected using Pan Tompkins algorithm implemented by Dr. Xavier L. Aubert. The two implementations were integrated in the set of PEF.

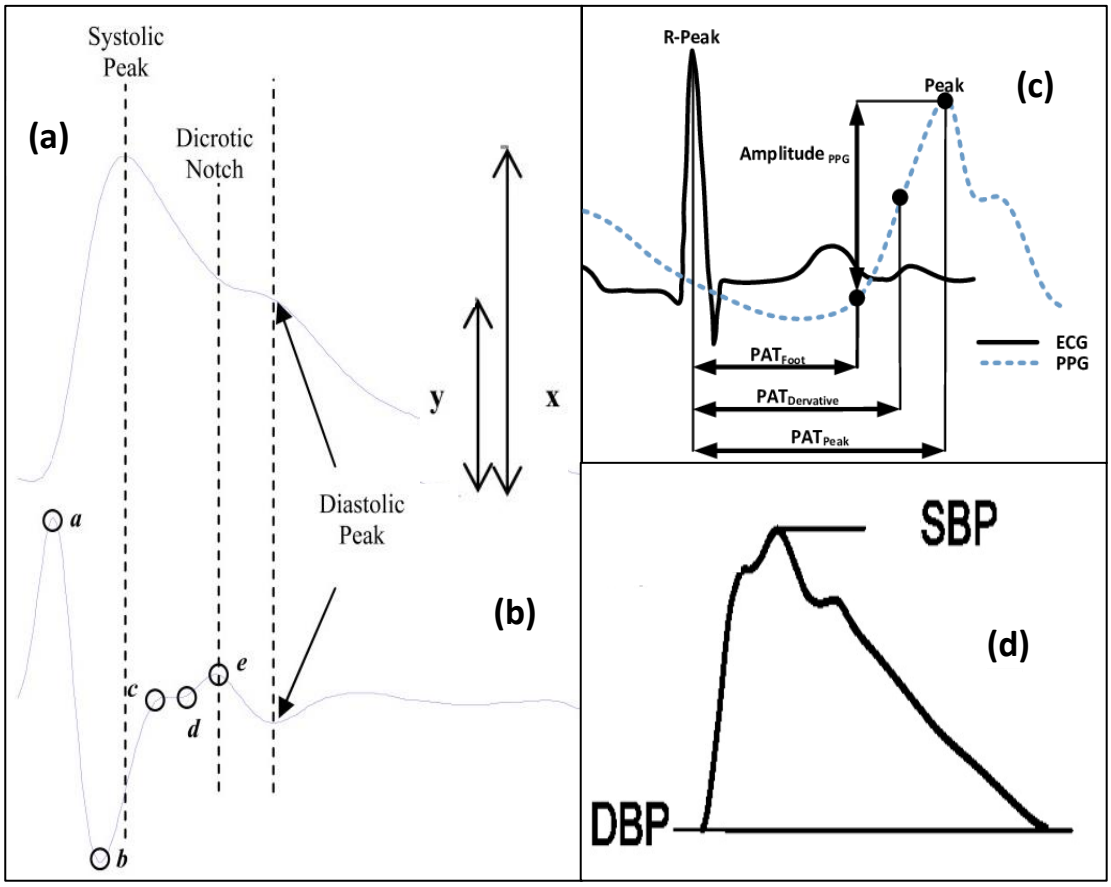

Figure 7: Explored biosignals waveforms with corresponding features representation (a) PPG AC component, (b) APG waveforms, (c) PAT different approaches and (d) BP waveform. Images adapted from [14], [50] and [51]. In (a), "y" corresponds to the amplitude of the diastolic peak (approximately equal do DN amplitude).

The two implementations were integrated in the set of PEF.

3.2.4. Manual noise detection

Undesirable loss of contact with the sensor or movements led to the appearance of noisy or absent regions in the collected signals. Also, PPG is subject to sudden amplitude changes due to the automatic gain controller in the amplifier of the PPG sensor [14]. So, in order to remove these low-quality segments, a strict manual analysis of the biosignals was performed. Since the automatic clearance of the biosignals was

not the main goal of this dissertation, the visual inspection was considered enough (figure 8).

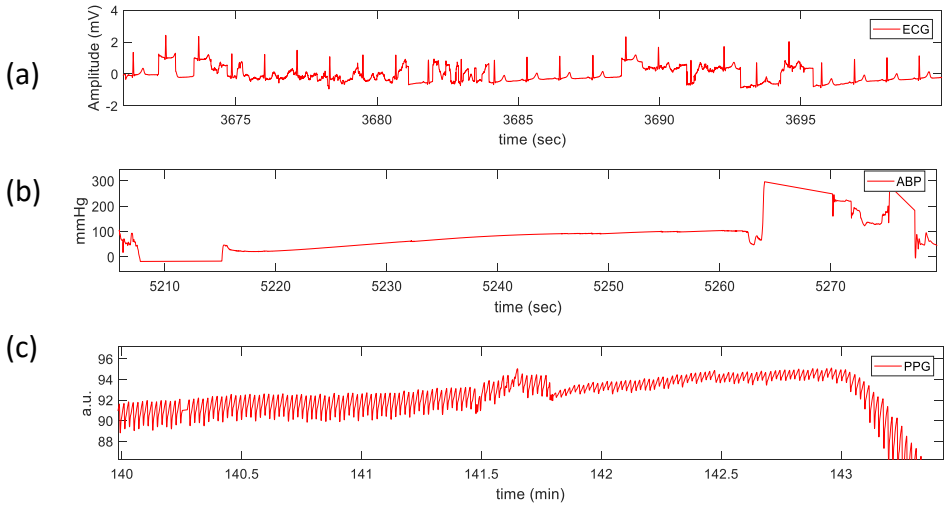

Figure 8: example of (a) noisy region in ECG and (b) absent and (c) low amplitude PPG at different times, for patient 1.

3.2.5. Moving average

The biosignals might still be blurred by motion resulting in high frequency artefacts. These artefacts' frequencies overlap with the PPG frequency range which results in significant relationships (between features) cover-up. So, in order to reduce it, moving average methods can be used [21]. This moving average was based on a causal filter, where each output depends on the past and present inputs. This means that each new sample will be the result of the average of the samples within the time span (which corresponds to the filter size) that precedes it (past inputs), including the sample in the issued time (present input). Figure 9 provides a graphical exemplification of this process for AC_A.

The filter's specifications might positively influence the expression of either steep or smooth features' variations throughout time. For instance, its size can neither be too small nor too big. Also, some percentage overlapping provides a greater number of measured samples and an adequate adaptation to the upcoming information, without

unwanted fluctuations. Therefore, it was defined windows of 10 seconds length with 50% overlapping.

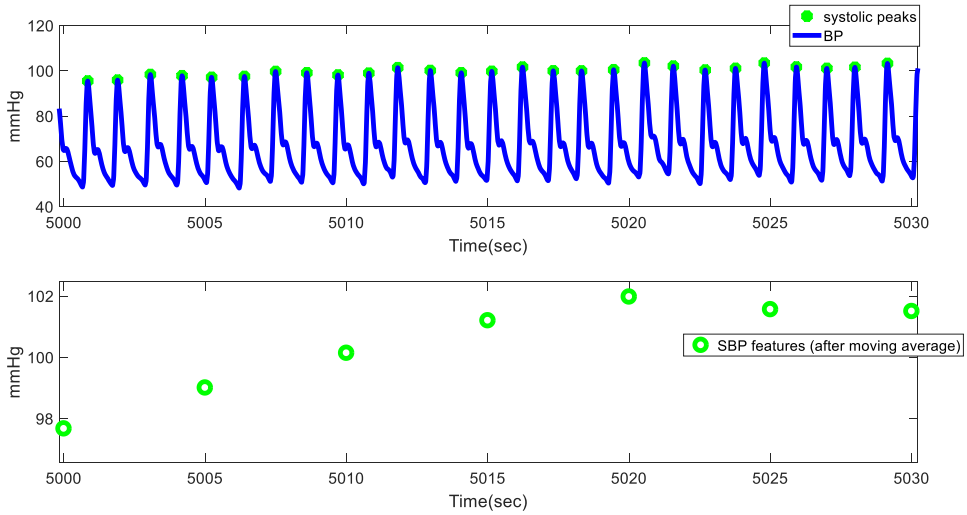

Figure 9: 27 BP events with the systolic points detected (upper panel) and SBP after moving average (lower panel). The filter's size is 10 seconds with an overlapping of 50%. As expected, the 30 seconds which are represented originate 7 samples, given the 5 seconds shift of the filter.

3.2.6. Strength of relationship between BPF and PEF

In order to inspect the relationship between BPF and PEF with more detail, the entire BP, ECG and PPG signals were segmented into fixed length non-overlapping windows or segments. Then, each window had the Spearman correlation coefficient (SCC) and linear regression coefficient (LRC) calculated for each variant from PEF against BPF. Figure 10 illustrates this situation with an example.

The correlation strength was evaluated according to the rule of thumb (table 3). LRC was instantiated in order to perceive if the prevailing variation in each window was positive (LRC>0) or negative (LRC<0).

The size of the considered windows has influence on the measurement of any existing strong relationship (depicted by SCC). On the one hand, each window has to be long enough so that it assembles a minimum number of samples that allow a valid

SCC calculation. On the other hand, excessively big windows need to be avoided, given that they might conceal any important pattern within features' comparative behaviour. So, values of 30 seconds, 1, 2 and 3 minutes were experimented

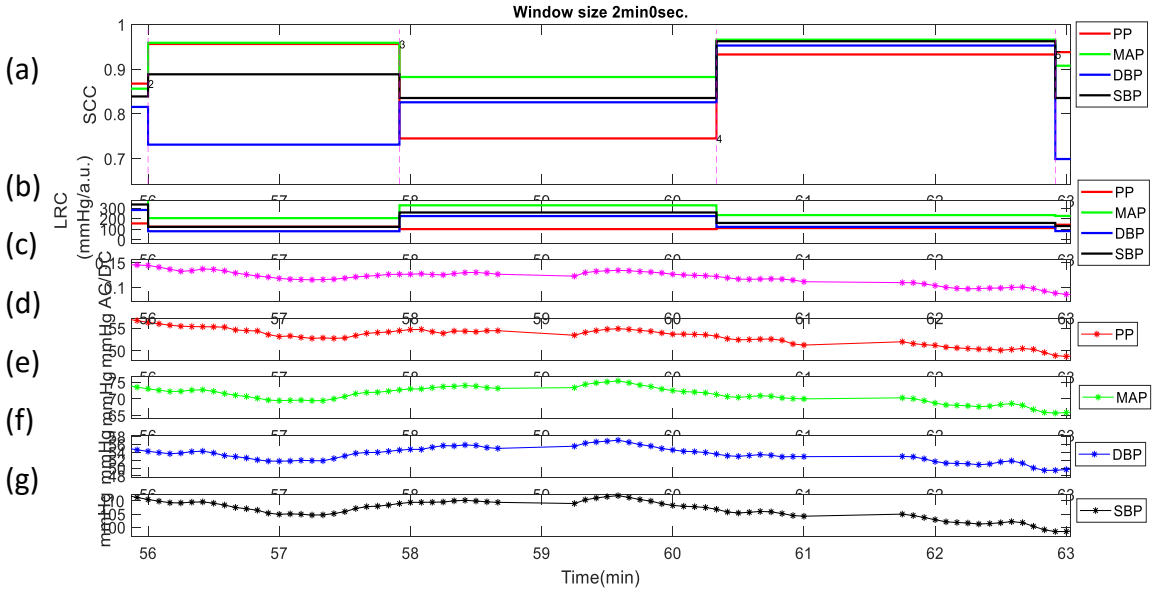

Figure 10: Three resulting consecutive windows with a length of 2 minutes each. (a) SCC, (b) LRC, (c) $\frac{AC_A}{DC_A}$ and (d), (e), (f), (g) BPF evolution (in mmHg). Each window appears separated by vertical pink dashed lines in (a) (labelled as "end"). Remark: the features' regions without dots (e.g. between minutes 61 and 62) correspond to excluded regions which were not regarded in the correlation in chapter 3.2.4.

Table 3: Correlation interpretation according to the rule of thumb. Source: [52]

Size of Correlation	Interpretation
.90 to 1.00 (−.90 to −1.00)	Very high positive (negative) correlation
.70 to .90 (−.70 to −.90)	High positive (negative) correlation
.50 to .70 (−.50 to −.70)	Moderate positive (negative) correlation
.30 to .50 (−.30 to −.50)	Low positive (negative) correlation
.00 to .30 (.00 to −.30)	negligible correlation

Furthermore, in order to analyse any determinant occurrences, every relationship had inspected the windows with an SCC above 70% (W70a). These segments manifest a (very) strong correlation, according to [52]. When compared with other segments

which possess an SCC below 70%, the probabilities of possessing interferences and no visible patterns are lower for W70a (figure 11).

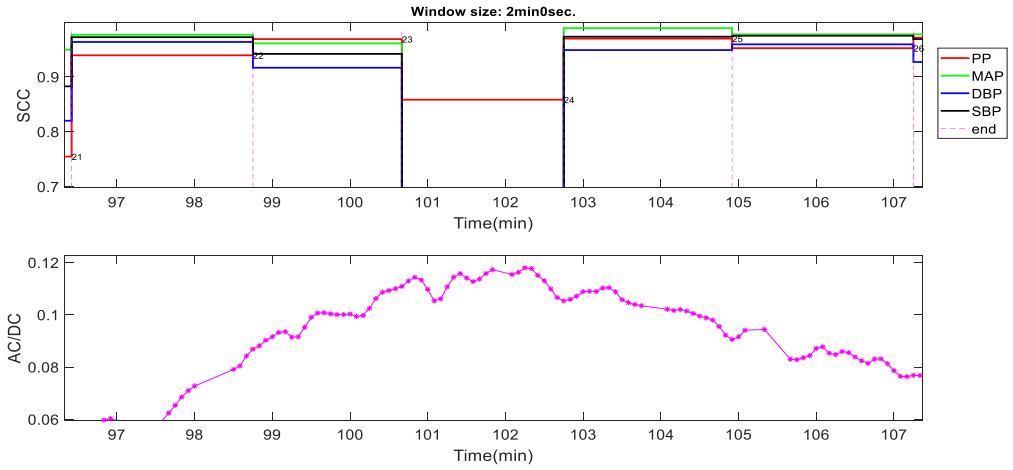

Figure 11: 5 consecutive windows with a length of 2 minutes each, separated by the vertical dashed lines (labelled as "end"). $\frac{AC_A}{DC_A}$ and respective SCC against MAP, SBP, DBP and PP are plotted. In this situation, only the third window in the depicted image approximately between 101 min and 103 min) was excluded from the analysis given that SCC<70% for SBP, MAP and DBP.

3.2.6.1. Incoherent relationship between BP and AC_A, DC_A and $\frac{AC_A}{DC_A}$

Under GA, BP and PPG are expected to behave as figure 12 depicts. The reported incoherencies in introduction between AC_A and MAP were inspected given the underlying information on ANB it might bring. In this situation, it was verified whether any of the concerned W70a had an SCC with an opposite signal from the majority of the windows. For instance, if the majority of the concerned W70a had a positive SCC but a small percentage exhibited a negative SCC, the segments corresponding to that small depicted percentage were put together and studied.

The exclusion from this analysis of other available segments showing unexpected relationships with weaker SCC was assumed. Only the strongly correlated segments were analysed given that they are associated to a more consistent relative evolution of

each pair of features. In other words, the depicted incoherencies are better delineated, correlated and less constrained by irrelevant sources of error.

The main objective of these reports was solely to highlight the existing inconsistencies separately for DC_A and AC_A. In its turn, the inclusion of $\frac{AC_A}{DC_A}$ was meant to test the influence that it could exert in these considered regions by combining the characteristics of DC_A and AC_A in a single feature. The fact that these incoherencies might weaken the correlations between PPG and BP was assumed.

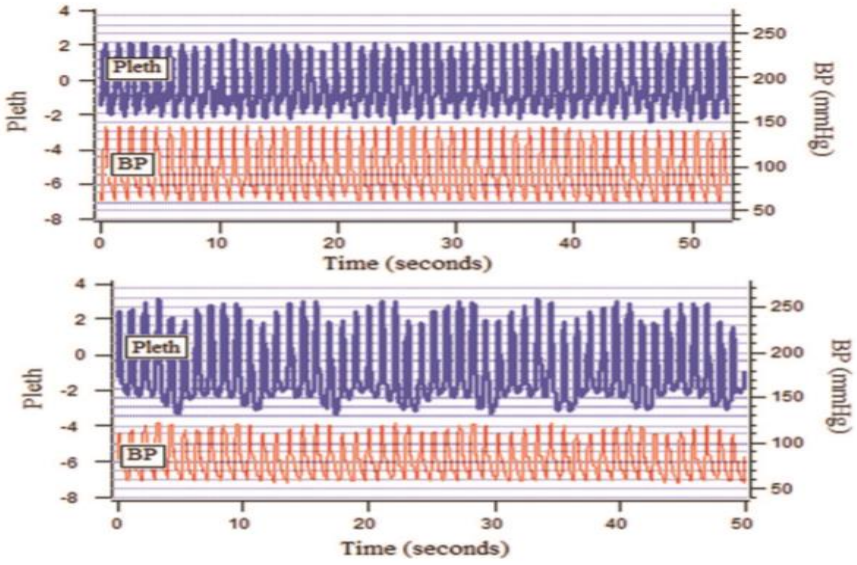

Figure 12: The graphs show the baseline waveforms of BP and PPG under anaesthesia (upper panel) and after loss of 1L of blood (lower panel). The lower graph depicts a small increase in the AC_A and a small decrease in MAP, as expected. Source: [15]

3.2.6.2. PEF performance assessment

Evaluation and comparison of the relationship of PEF against each feature from BPF. This performance assessment was divided in two stages.

On the one hand, it was calculated the SCC between each separate feature from BPF and the corresponding PEF, for each patient. It was considered the extracted features from the entire surgical procedure. This enabled the general inspection of the relationships between the different features.

On the other hand, due to the small number of patients and in order to address the varying correlation performance between features throughout the entire procedure, it was considered the segmentation of the biosignals (in 2 minutes segments). This was followed by the calculation of the SCC for each segment between PEF and BPF. It was separately assigned for each patient the relationship which could provide the bigger number of strongly correlated segments to each BP feature. The selected relationship was addressed in the BP assessment stage that follows. Boxplots of the full set of SCCs were drawn and the corresponding Median, Interquartile range (IQR) and disparity of the outliers were registered for each evaluated relationship. These metrics are not as influenced by outliers as other performance indicators, such as the Mean. This means that a bigger Median and smaller IQR provide an unbiased big quantity of strongly correlated segments to be assembled.

3.2.7. BP assessment

It is required to announce beforehand that in this stage the same segmentation of the biosignals was done and that the size of each window was set to 2 minutes, in order to enable further analysis.

Regarding the methodology itself, firstly a normalization of all features was done by computing z-score. This scaling procedure subtracts the mean of the full range of values from those values and divides this difference by their standard deviation. If the features' scales are wildly different, this might have a knock-on effect on the model. Then, it was tested the ambiguity among the PEF, based on the Kruskal wallis test. Its null hypothesis states that the concerned features come from the same distribution. If this is rejected, it means that there are significant differences among the features and that they can be incorporated as assets in the features' set. This validates the non-ambiguity in PEF.

Furthermore, based on a leave-one-out cross validation, it was assessed the BP for the full time of the surgical period in the one patient that represents the validation set. For that end, parameters were arranged, for each feature from BPF, through MLR, as the equation 8 illustrates for MAP assessment:

$$MAP = cte + p_1 * \frac{AC_A}{DC_A} + p_2 * AC_A + p3 * DC_A + p4 * HBI + p5 * DN + p6 * \frac{B}{A} + p7 * RI + p8 * PAT_1 + p_9 * PAT_2 \quad \ldots(8)$$

, where p_n, n∈[1:9] are the resulting parameters from MLR and cte is a constant.

Regarding the computed models, different characteristics were explored. Each model held a distinguishing characteristic, compared to the "reference" computed Model (M1), in order to evaluate the influence of its inclusion in the concerned model.

Firstly, the influence that the selection of certain parts of the biosignals (instead of the full biosignals) could have on the model was addressed (M2). For this end, it was regarded "every window with an SCC>70%, concerning the variant from BPF that is being assessed and the associated best correlated variant from PEF" (W70b), according to the performed task in chapter 3.2.6.2. To exemplify this situation: if $\frac{AC_A}{DC_A}$ is the best performing variant against MAP, the model on the MAP assessment will assemble every segment of the biosignal whose SCC, concerning MAP and $\frac{AC_A}{DC_A}$, is above 70%.

Parameters were also arranged without PAT_2 in order to test its influence (M5). PAT_2 holds a great performance review but still requires an ongoing intervaled calibration throughout the entire procedure which is not time-effective. This might have effects on the surgical agenda.

Also, to avoid the extra setting of ECG electrodes (for PAT estimation) a model was elaborated and evaluated without the PAT_1 and PAT_2 (M6). The implementation of its sensors takes essential operational time.

When it comes to reduce the influence that interpatient variability has on similar BP estimation's systems, initial calibrations are usually addressed. These calibrations are associated to a small period of time (before surgery begins) where the models' parameters are updated with the collected data from the patient under surgery. This procedure delays the beginning of the surgery. Therefore, an initial calibration procedure was suggested and its influence was addressed on the BP assessment in two models (M3 and M4). Here, the built model involved two separate stages. Firstly, MLR was implemented on the training set data (similarly to the previous situations). Then, the resulting parameters from the first stage were modified on the calibration 2 minutes period (a total of 23 features samples) through a recursive least squares (RLS) method (equation 9). This algorithm is recognized for its fast convergence rate. The selected estimation method of RLS was the forgetting factor (). The smaller is, the more sensitive to recent samples the filter is, which causes more fluctuations in the filter coefficients. In practice, is usually between 0.98 and 1, so it was selected 0.99. [53]

$$y(t) = a_1 * u(t) + a_2 * u(t-1) \quad (9)$$

, where u(t) and y(t) are the real-time input and output data, respectively. a_1 and a_2 are the parameters for the real time and past inputs, respectively.

Overall, the disregard of ECG and calibrations streamlines the entire clinical procedure and contributes for patient comfort.

The major role that $\frac{AC_A}{DC_A}$ might have in BP assessment was also tested through the implementation of a model to which was removed $\frac{AC_A}{DC_A}$ (M7). The performance of the considered models was evaluated in a two-steps procedure. All the implemented and tested models are described in figure 13.

The built models were separately evaluated for each patient through the computation of the SCC and RMSE between the estimated BPF (in the considered models) and the real BP measurements. The undertaken interpretation was meant to highlight the model which met the best SCC and RMSE values for all the BPF, if possible. The small used dataset allowed this more exhaustive individual analysis of each patient. Then, it was calculated the mean SCC and mean RMSE, regarding the three patients, which enabled to decide what the best implemented model was.

Moreover, the agreement between the real and estimated BPF was measured based on two different protocols of requirements from the British Hypertension Society (BHS) and the Association for the Advancement of Medical Instrumentation (AAMI)

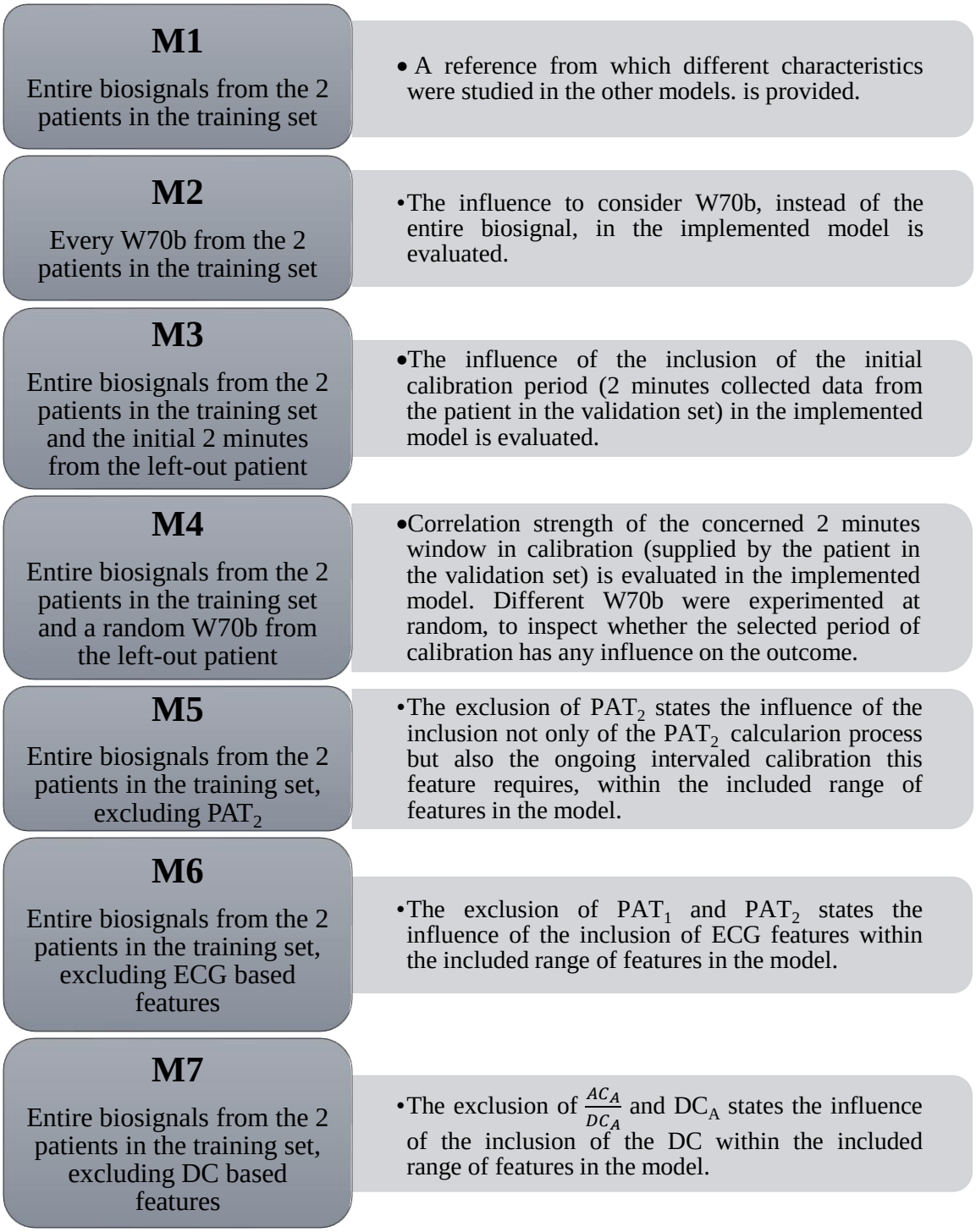

Figure 13: Schematic description of the different implemented models.

Firstly, based on the BHS protocol for evaluating (semi-) automatic blood pressure recording systems, a nonparametric method (BHS_{np}) is recommended. It avoids the negative impact that extreme discrepancies between measurements might have [38]. According to BHS_{np}, any measurement system may be classified as A, B, C, D depending on the percentage of the differences between the real and the estimated BPF values (DIFF) that fall within 5,10,15 mmHg, as the table 4 shows.

Table 4: Grading of the BP assessment system according to the non-parametric approach of BHS. Source: [54]

	Difference (mmHg)		
Grade	≤5	≤10	≤15
A	60	85	95
B	50	75	90
C	40	65	85
D	fails to achieve C		

This classification grading requires all the three percentages from table 4 to be exceeded or at least matched, being A the best grade to be reached. So, for example if a device is A graded, it means that the percentages of the DIFF within 5, 10 and 15 mmHg were equal to or bigger than 60%, 85% and 95%, respectively.

The mean DIFF ($\overline{DIFF}$) and standard deviation of DIFF (SD) were also determined in order to assess whether the implemented model is within AAMI recommendations which require $\overline{DIFF} \leq 5$ mmHg and SD ≤ 8 mmHg.

To assist the analysis, the Bland-Altman plots were drawn for each estimated BP feature [54,22]. The best performer is selected within these standards which have been validated as such in the scientific community.

4

Results and discussion

4.1. SPI and ANI computation

In the end, no reliable correlation was obtained between the BP features and any of the computed indexes. These negligible correlations might have been related with both implementation and data quality challenges.

Both SPI and ANI implementations demand the acquisition of the processed algorithm from the manufacturer. The publicly available information on these algorithms is ambiguous and scarce when it comes to the concerned details of calculation. Namely, both these indexes require a normalization procedure which is not totally explained in the original documentation. On the one hand, the feature scaling of the obtained RR series values between -0.1 and 0.1 are not referred. A min-max normalization was implemented as alternative. On the other hand, SPI histogram transformation concerns a combination of both group and individual distributions which is considered to be misleading. Its mean arrangement's description ("mean of the distribution is defined as the mean of the measured data" [8]) seems to dismiss any information from the group distributions (contrarily to the weighted combination referred in chapter 3.2.1.). In this situation, the mean of the combined distribution was a result of the weighted means of each distribution, as referred in chapter 3.2.1. . Even though the obtained negligible correlations couldn't clarify any sort of relationship between these indexes and BP, the alternative solutions were considered to devaluate the resulting conclusions.

Regarding SPI training group, the smaller number of included patients in this initial study (18), compared with the 72 from [8], is more predisposed to cause overfitting. This problem wasn't verified for ANI since it is not dependent on any training group.

Besides the implementation's struggles, the data from MIMIC II was also associated with some drawbacks such as missing data, patient movement, human and transmission errors and sensor degradation which were observed in practice [55].

In order to confirm the origin for the obtained negligible correlations between BP and the computed ANI and SPI, both implementations should be validated against the certified algorithms. Once again, the absence of any results in this stage doesn't

compromise the proposed objectives since this dissertation wasn't meant to reach any conclusive results about the performance of SPI and ANI.

4.2. Features extraction

The peaks' detection was visually inspected and successfully validated. Figure 14 depicts a singular event, for each biosignal, with all the corresponding peaks in the expected locations, as it was generally observed. On the rare occasions it failed (due to PVC, for example), that part of the biosignal was removed from the analysis.

SBP and DBP corresponding peaks were detected based on their concavity. They are highest and lowest values, respectively, in a BP event. AC systolic peak and DC diastolic and systolic peaks were also detected given their prominence in a single event. The AC systolic and diastolic peaks detection enabled to pinpoint the location of 20% AC amplitude, computed according to the provided method of [46]. The "diastolic" peak, as [14] denominates it (depicted in figure 14 for AC), was determined based on the APG and its approximation to 0 (with the apriori knowledge that its location is expected to be after the DN). "b" and "a" waves from APG were detected based on the provided information by [56] which explored their concavity. According to DN and "e" wave share the same position (according to [57]). Therefore, the concavity of the "e" wave enabled DN precise identification.

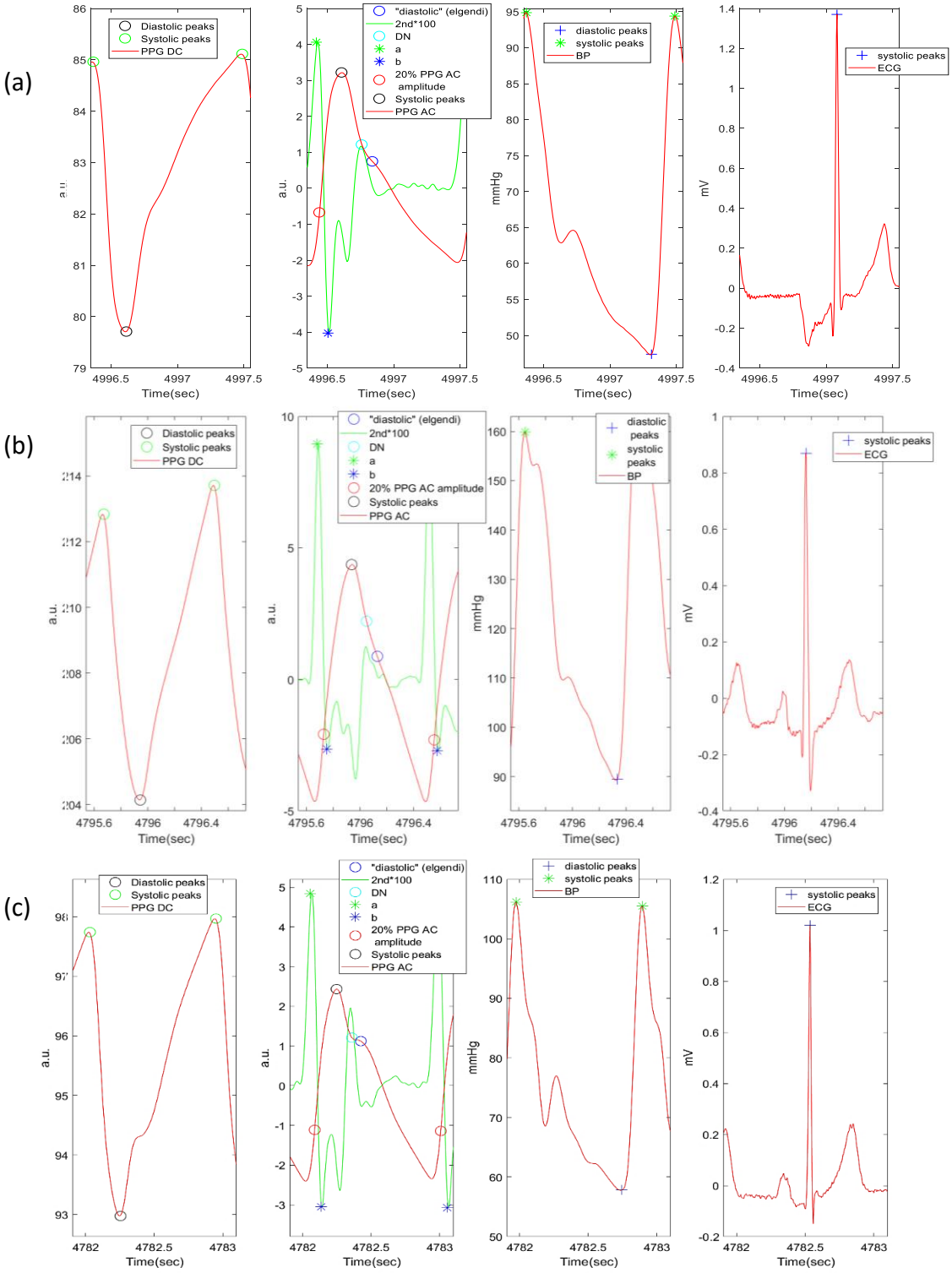

Figure 14: Patient 1 (a), 3 (b) and 5 (c) DC, AC, ECG, and BP (from left to right) with the respective detected points and corresponding labels. These detected points are on the basis of the PEF and BPF calculation.

During the validation of the features extraction, some variability was observed in the waveforms of AC which might have consequences in the stages that follow. In patients 1 and 5, a better delineated dicrotic notch was noticeable, when compared with patient 3 (figure 14). On this topic, the vessels' stiffness was reported to increase with age and cardiovascular peculiarities [58,14], namely through observations of the shortening of the reflected PPG wave's arrival time. In its turn, this is responsible for a less clear DN location in aged people when compared with young and middle-aged patients which complicates its precise detection (figure 15). It is possible to observe the close relationship in the AC waveforms on the one hand between both patients 1 and 5 and the depicted PPG event in figure 15.a and on the other hand between patient 3 and the depicted event in figure 15.b.

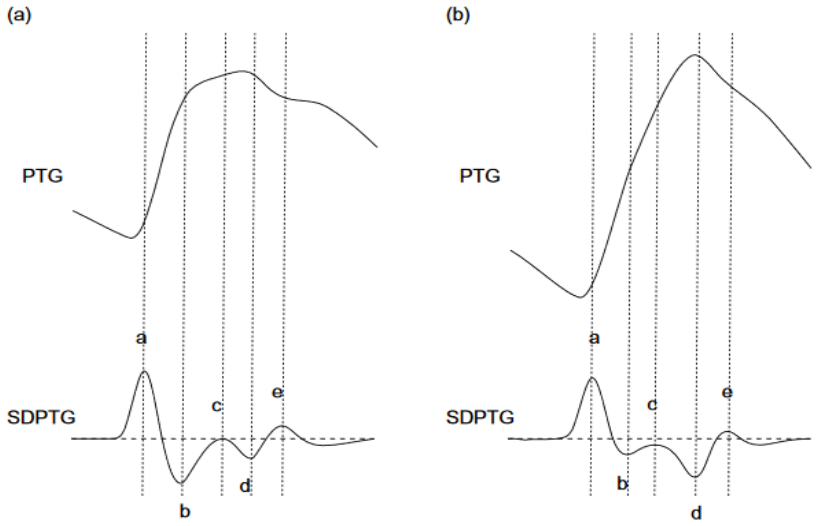

Figure 15: Representative recordings of one PPG, and corresponding APG (SDPTG in the figure), event waveform from 39-year-old (a) and 82-year-old subjects (b). Source: [24]

APG is also known to correlate with age (and corresponding cardiovascular health), whose waveform changes accordingly (figure 16). This relationship can be comprehended through the variant $\frac{B}{A}$ [24,14]. In [42], $\frac{B}{A}$ was reported to be negatively correlated with age. So, in order to explain the differences in the waveforms, that same analysis of $\frac{B}{A}$ was done. The $\frac{B}{A}$ mean values from patient 1 and 5 were 0.83 and 0.75, respectively, which in its turn were higher than those from patient 3, equal to 0.35.

These results combined with the AC waveform similarities description confirms the literature.

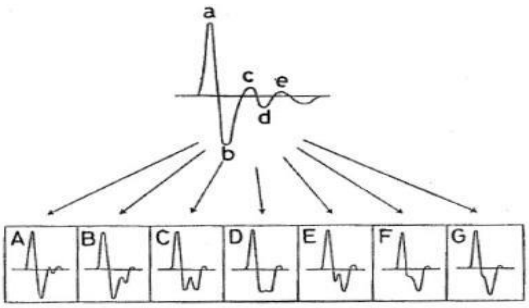

Figure 16: APG waveform associated to good circulation (A) and bad circulation (G), with the in-between intermediate states. It is noticeable the decreasing amplitude of the "b" wave (from (A) to (G)). Source: [14]

4.3. Incoherent relationship between AC_A, $\frac{AC_A}{DC_A}$ and DC_A with BPF

As reported by Dr. Jens Muehlsteff, inconsistent behaviour between BP and PPG was observed. After the inspection of the biosignals for the 3 patients, the W70a with inconsistent behaviour were depicted in terms of percentages, from the entire collected biosignals (table 5). For patients 1, 3 and 5, the entire biosignals correspond to 64, 84 and 67 segments (of 2 minutes each), respectively.

Table 5: Percent representation of the depicted W70a with unexpected relative behaviour between BP features and AC_A, $\frac{AC_A}{DC_A}$ and DC_A, for each patient.

	Patient 1	Patient 3	Patient 5
AC_A	5 %	1 %	15 %
DC_A	0 %	7 %	0 %
$\frac{AC_A}{DC_A}$	5 %	4 %	9 %

Focusing on the comparative inspection of AC_A, DC_A and $\frac{AC_A}{DC_A}$, DC_A null percentage values for patients 1 and 5 depict not only the consistency of this feature but

also the fact that all the regions that contributed to the observed unexpected behavior from $\frac{AC_A}{DC_A}$ were due to AC_A (since no synergetic effect was observed). Also, the percent decrease from AC_A to $\frac{AC_A}{DC_A}$ in patient 5 shows the decisive improvements that the latter brings when compared to the former. These associations were not depicted for patient 3, though. However, the percentage of W70a (from the entire biosignals) depicting the expected relationships between features for patient 3 was much lower than those values presented for patients 1 and 5. After analysis of all BPF, these percent values for patient 3 varied between 25% and 48% while for patients 1 and 5 these percentages ranged between 70% and 86% and between 60% and 90%, respectively. So, the associated results to patient 3 in this chapter lost their relevance.

An example, from patient 5, of the inconsistent behaviours between features is shown in figure 17. Both for $\frac{AC_A}{DC_A}$ and AC_A, nearby minutes 26 and 29, it is observed a curve with positive concavity, whereas for SBP, DBP and MAP it is notorious a curve with negative concavity. Also, from minute 30 and in the 3 minutes that follow it, BPF decrease is accompanied by an AC_A and $\frac{AC_A}{DC_A}$ increase. The depicted occurrences resulted in a strong negative correlation (SCC < -0.7), which is inconsistent with the mainly observed positive correlation in the entire biosignal.

In minute 25, it is depicted a situation where the $\frac{AC_A}{DC_A}$ outperforms AC_A in terms of correlation performance. The observed unexpected curvy event for AC_A led to an SCC close to -0.8 with MAP, DBP and SBP. However, this curve was softened for $\frac{AC_A}{DC_A}$ which enabled the decline of the observed correlation (first window of figure 17.a and 14.b). The representation of the SCC between 0.7 and 1 in figure 17.c for the same considered time period in figure 17.a and 17.b depicts no unexpected relationships for DC_A.

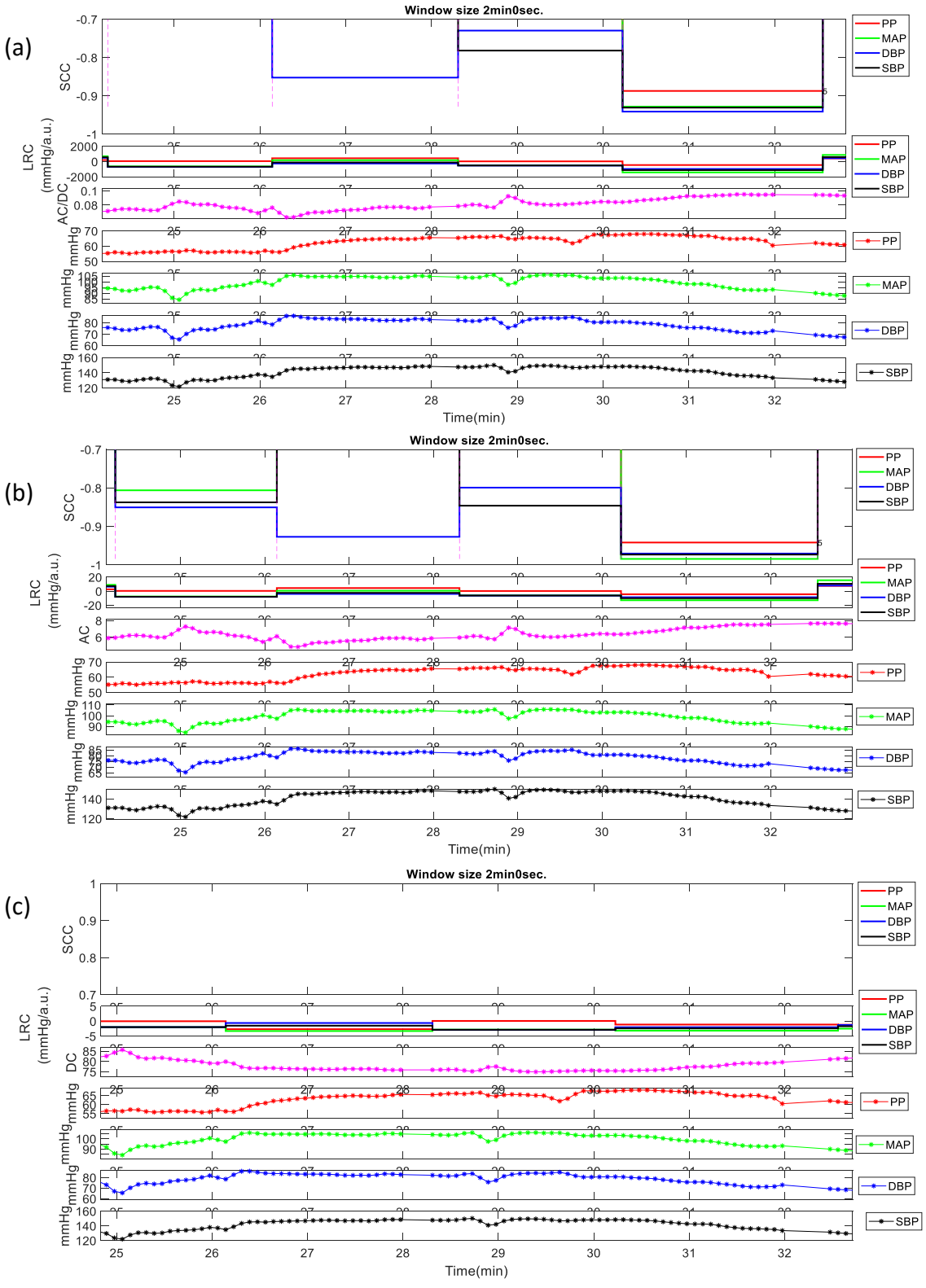

Figure 17: set of 4 consecutive W70a, in the same time span, concerning BPF against $\frac{AC_A}{DC_A}$ (a), AC_A (b) and (c) DC_A. It is hereby depicted an unexpected relationship of AC_A and $\frac{AC_A}{DC_A}$ with MAP, SBP and DBP which is not followed by DC_A.

So, it is considered that DC exerts a positive influence towards BP assessment whereas the observed unexpected relationships between AC based features and BP rather point out for a complementary action towards the systemic vascular activity description. The $\frac{AC_A}{DC_A}$ allowed to avoid only 6% of the observed inconsistencies for AC_A

Also, the possibility that these incoherencies weaken the relationship between PPG and BP was disregarded. Even though the observed incoherencies varied between 5% and 15% for AC_A and $\frac{AC_A}{DC_A}$ in patients 1 and 5, for DC_A the percentage values remained null for both patients as well which in its turn is considered to compensate.

Further and more precise explanations for these inconsistent events can't be extrapolated based on the scarce existing information on the surgical procedure (e.g. description of events) as well as the complexity of this system. Also, in order to have a more extensive statistically valid understanding of these dynamics, more patients should be involved or new requirements should be established (e.g. consider segments with SCC > 50% instead of the W70a) in order to assemble a bigger number of use cases.

4.4. PEF performance assessment

From the drawn boxplots, it is noticeable the number of several outliers (red dots after the end of the whiskers in figure 18, which correspond to the segments whose SCC is detached from the vast majority (within the whiskers). Nevertheless, the reduction of their influence by addressing median and IQR was assured. Once again, the estimation of these metrics' values had the only purpose to find for each patient, the features from PEF with the biggest number of well correlated segments with each feature from BPF.

For instance, in patient 1, $\frac{AC_A}{DC_A}$, AC_A, DC_A and DN had some visible outliers. However, their high median and small IQR show the relatively small percentage that these outliers represent, within the entire set of segments. In this sense, the mentioned features provide a larger amount of strongly correlated segments than PAT_2 which has a smaller SCC and higher IQR. A more validated metric could have been used, such as the SCC, but an unbiased result wouldn't be obtained. For example, even though for patients 1 and 5 the features PAT_2 and $\frac{B}{A}$ were shown to be strongly correlated with

most of the BPF (91>SCC(%)>70), the associated high IQR values (0.63>IQR>1.22) demonstrates the broad range of obtained segments.

In order to have a more accurate reading of the median and IQR values, table 6 was elaborated with the precise corresponding values for each patient. From this analysis, it was chosen for each patient the feature from PEF which was the best related with each feature from BPF, as previously mentioned. The selected features presented the highest median and the lowest corresponding IQR values. Therefore, in patient 1 the BPF were associated with $\frac{AC_A}{DC_A}$. Patient 3 had MAP, SBP and PP associated with $\frac{B}{A}$, and DBP with AC_A. Patient 5 had MAP, SBP and DBP associated with DC_A and PP with $\frac{AC_A}{DC_A}$.

In terms of the calculated SCC, patient 3 only presented strong correlations for PAT_2 and $\frac{B}{A}$ (except for PP_3) while the remaining features from PEF had negligible to moderate correlations. The good performance of these two features, which is observed across all patients, needs to be highlighted since their relationship with BP features surpasses the identified physiological differences from patient 3 to patients 1 and 5. Firstly, based on the relationship that $\frac{B}{A}$ is known to have with arterial stiffness, it is corroborated the decisiveness of this physiological characteristic on the differentiation of the patients. Even though the relationship between BP and PAT is known to be dependent on vascular properties (e.g. vessel radius, vasomotor tone) [19], the frequent calibration of PAT_2 managed to overcome this dependency. In contrast, the bad performance from PAT_1, which doesn't hold any calibration, emphasizes this aspect.

.

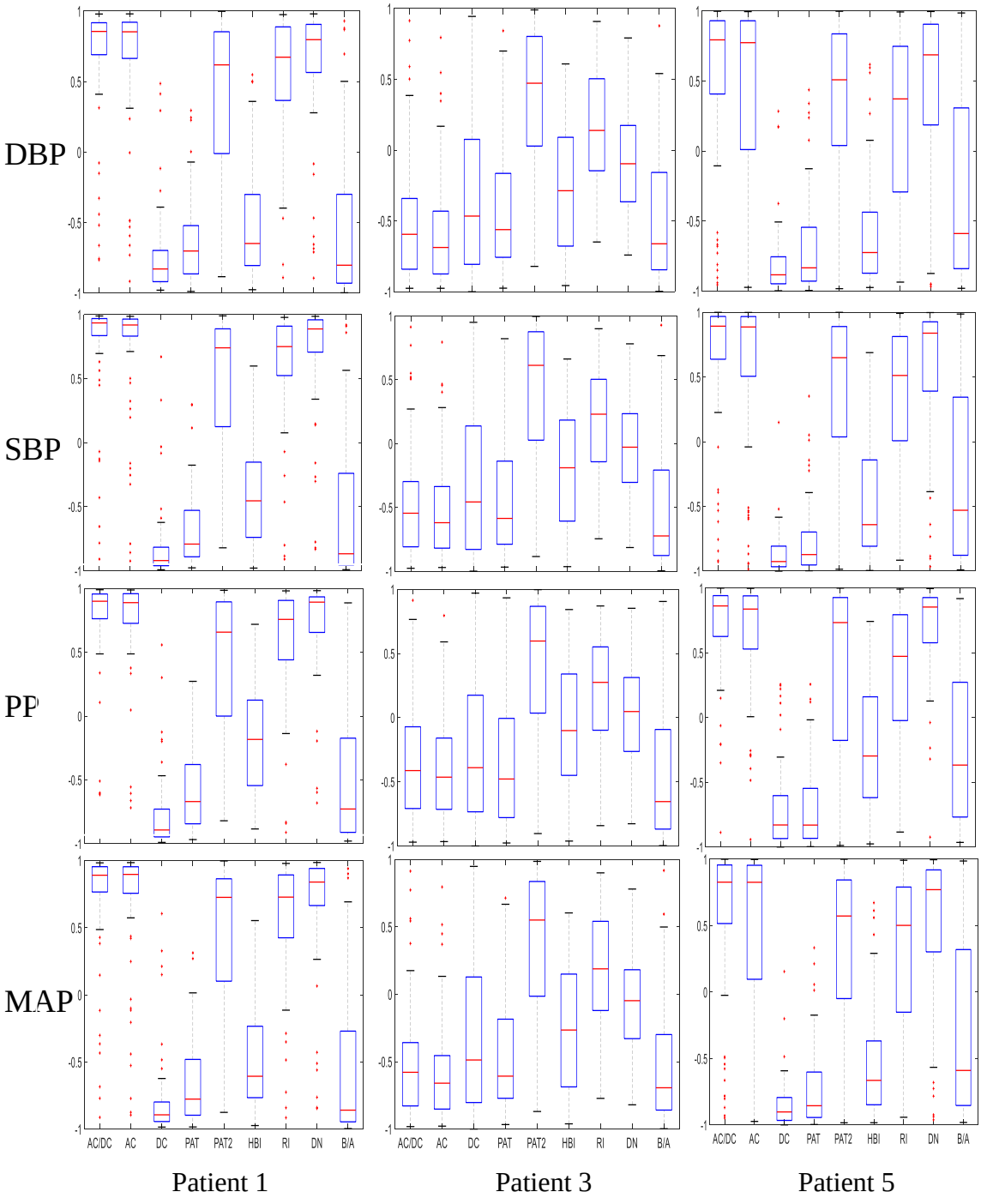

Figure 18: boxplots of BPF set of *SCCs* (yy-axis) against PPG and ECG features (xx-axis). For patient 1,3 and 5, it was assembled 64, 84 and 67 segments (of 2 minutes each), respectively. The boxplots were based on the set of these segments.

Furthermore, in patient 3, the SCC of AC_A and $\frac{AC_A}{DC_A}$ actually had opposite signals when compared with patients 1 and 5. This corroborates the previously raised inconsistent behaviour of AC_A and $\frac{AC_A}{DC_A}$ for patient 3 in chapter 4.3.. Therefore, in the analysis that follows, it is always inspected how relevant the exclusion of patient 3 is for the results.

Furthermore, for both patients 1 and 5, HBI was the worst performing feature, with both positive (SCC (%) <16) and negative (SCC (%) <58) negligible to moderate correlations. These poor results are due to the fact that changes in HBI are known to be associated with the heart activity rather than the vascular properties to which BP is intimately related with. PAT_1 was strongly correlated only for patient 1 while the vascular conditions of patient 5 might have contributed for the less successful correlation performance of this feature. Apart from HBI and PAT_1, in general, the correlation performance of PEF with any of the features from BPF was strong, with the only exception for PP. For instance, both PP_5 and PP_1 was outperformed in terms of their SCC with PEF by the other BP features.

At last, concerning the highlighted features in this dissertation, PAT_1 and PAT_2 had similar correlational performances to $\frac{AC_A}{DC_A}$ and DC_A with BPF for patient 1 but couldn't manage to follow that same accuracy for patient 5. PAT_1 was fairly inconsistent ($12 < SCC\ (\%) < 76$) while PAT_2 was outperformed by $\frac{AC_A}{DC_A}$ in terms of SCC for all the BPF.

Table 6: Median (IQR) of the set of segments (1-$\frac{AC_A}{DC_A}$, 2-AC_A, 3-DC_A, 4-PAT_1, 5-PAT_2, 6-HBI, 7-RI, 8-DN, 9-$\frac{B}{A}$). MAP_x, SBP_x, PP_x, DBP_x where x is the number of the patient.

	MAP_1	SBP_1	PP_1	DBP_1	MAP_3	SBP_3	PP_3	DBP_3	MAP_5	SBP_5	PP_5	DBP_5
1	0.9 (0.19)	0.93 (0.13)	0.9 (0.19)	0.86 (0.23)	-0.57 (0.47)	-0.55 (0.51)	-0.41 (0.64)	-0.59 (0.5)	0.88 (0.46)	0.89 (0.28)	0.83 (0.27)	0.82 (0.64)
2	0.9 (0.2)	0.92 (0.13)	0.89 (0.23)	0.85 (0.26)	-0.66 (0.4)	-0.62 (0.48)	-0.46 (0.56)	-0.69 (0.44)	0.83 (0.65)	0.88 (0.47)	0.81 (0.3)	0.79 (0.76)
3	-0.89 (0.15)	-0.92 (0.14)	-0.89 (0.22)	-0.83 (0.22)	-0.49 (0.93)	-0.46 (0.96)	-0.39 (0.91)	-0.47 (0.88)	-0.9 (0.16)	-0.91 (0.15)	-0.79 (0.37)	-0.87 (0.18)
4	-0.78 (0.42)	-0.79 (0.36)	-0.67 (0.46)	-0.7 (0.34)	-0.61 (0.59)	-0.59 (0.65)	-0.48 (0.78)	-0.56 (0.59)	-0.84 (0.31)	-0.86 (0.26)	-0.83 (0.28)	-0.81 (0.35)
5	0.73 (0.76)	0.74 (0.76)	0.66 (0.9)	0.62 (0.86)	0.55 (0.85)	0.61 (0.85)	0.6 (0.83)	0.47 (0.77)	0.51 (0.93)	0.62 (0.92)	0.71 (1.02)	0.45 (0.89)
6	-0.61 (0.53)	-0.45 (0.59)	-0.18 (0.67)	-0.65 (0.5)	-0.27 (0.84)	-0.19 (0.79)	-0.1 (0.79)	-0.29 (0.77)	-0.63 (0.4)	-0.57 (0.46)	-0.32 (0.66)	-0.67 (0.37)
7	0.73 (0.47)	0.75 (0.39)	0.76 (0.47)	0.67 (0.52)	0.19 (0.66)	0.23 (0.65)	0.27 (0.65)	0.14 (0.65)	0.41 (1.19)	0.38 (1.16)	0.46 (0.94)	0.39 (1.2)
8	0.84 (0.28)	0.89 (0.25)	0.89 (0.28)	0.8 (0.34)	-0.05 (0.51)	-0.02 (0.54)	0.05 (0.58)	-0.1 (0.54)	0.79 (0.59)	0.84 (0.49)	0.83 (0.32)	0.73 (0.67)
9	-0.86 (0.68)	-0.87 (0.71)	-0.73 (0.74)	-0.8 (0.63)	-0.69 (0.56)	-0.72 (0.67)	-0.65 (0.78)	-0.66 (0.69)	-0.58 (1.22)	-0.5 (1.22)	-0.37 (1)	-0.62 (1.19)

Table 7: SCC considering the entire signal (1-$\frac{AC_A}{DC_A}$, 2-AC_A, 3-DC_A, 4-PAT_1, 5-PAT_2, 6-HBI, 7-RI, 8-DN, 9-$\frac{B}{A}$). MAP_x, SBP_x, PP_x, DBP_x where x is the number of the patient.

	MAP_1	SBP_1	PP_1	DBP_1	MAP_3	SBP_3	PP_3	DBP_3	MAP_5	SBP_5	PP_5	DBP_5
1	0.86	0.86	0.79	0.85	-0.32	-0.3	-0.23	-0.33	0.9	0.93	0.77	0.86
2	0.79	0.79	0.74	0.79	-0.54	-0.53	-0.43	-0.52	0.84	0.9	0.8	0.79
3	-0.92	-0.9	-0.8	-0.92	-0.57	-0.57	-0.42	-0.56	-0.86	-0.79	-0.48	-0.89
4	-0.83	-0.87	-0.92	-0.78	-0.38	-0.43	-0.47	-0.34	-0.23	-0.41	-0.76	-0.12
5	0.9	0.9	0.86	0.88	0.82	0.82	0.6	0.8	0.76	0.8	0.7	0.71
6	-0.55	-0.51	-0.41	-0.58	0.11	0.04	-0.16	0.16	0.09	-0.05	-0.37	0.16
7	0.8	0.79	0.71	0.8	0.56	0.55	0.4	0.57	0.80	0.70	0.34	0.84
8	0.79	0.79	0.73	0.78	0.33	0.28	0.06	0.37	0.91	0.93	0.73	0.88
9	-0.91	-0.9	-0.83	-0.9	-0.81	-0.77	-0.48	-0.82	-0.77	-0.75	-0.51	-0.77

4.5. Kruskal wallis

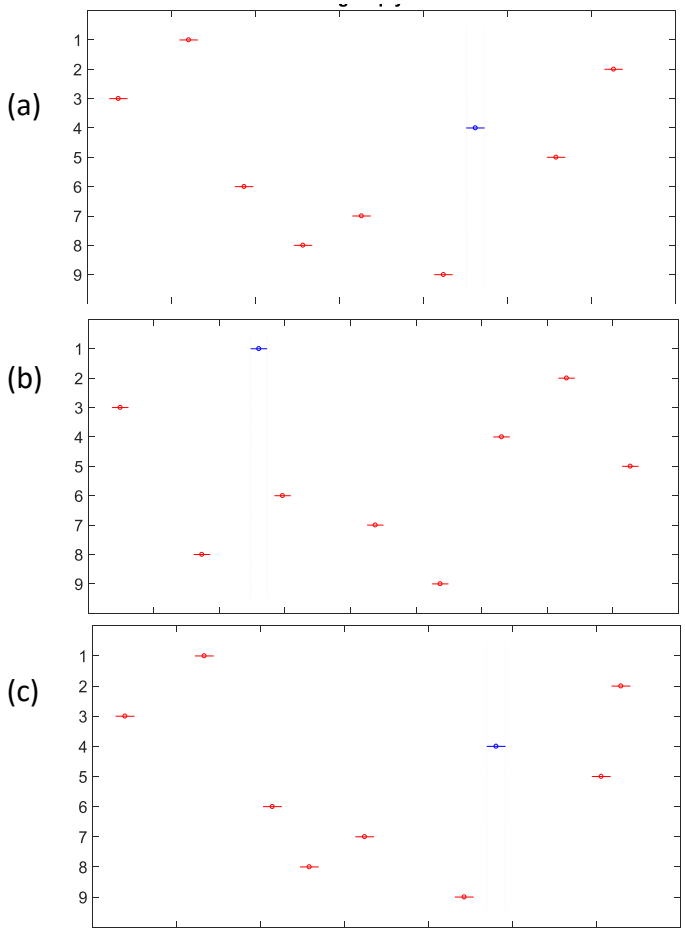

Figure 19: Kruskal wallis test graphical representation for patient 1 (a), 3 (b) and 5 (c). The function that enabled to plot these graphs was provided by MATLAB and didn't allow to zoom in. yy-axis: BP studied features.

In order to better perceive the outcome of this test, the results are hereby graphically represented in figure 16 for each patient. Two group means are significantly different (and non-ambiguous) if their intervals are vertically disjoint; which means the implied null hypothesis from this test is rejected. The three graphs from figure 19 show that none of the considered features was ambiguous, for any of the patients. Therefore, all the extracted features from PPG and ECG were used in the regression model.

4.6. Models' evaluation in terms of SCC and RMSE

Regarding figures 20 and 21, the various addressed models were compared in terms of the resulting SCC and RMSE between the estimated and the real BPF. First of all, for patient 3, all the models presented at best a moderate SCC. Despite M4 indicated strong correlations for DBP, SBP and MAP, their RMSE was distinctively high. For the same patient 3, M3 had a moderate SCC for all BPF but an inconsistent behavior for patients 1 and 5. On the one hand, for patient 1, the estimation of PP was strongly correlated with the real PP (SCC between 0.85 and 0.9), on the other hand, for patient 5, PP was the worst feature to be assessed (SCC close to 0.2), but SBP, DBP and MAP clearly improved (SCC > 0.8). The small quantity of data provided from the patient in the validation set (23 samples) might have been one of the reasons for the reported inconsistent results. In terms of the studied models, each BP estimated feature was separately considered for each patient. In this scenario, the best performer couldn't be visually perceived since the SCC and RMSE values were very similar. If it had to be highlighted one model though, M2 would be the selected, with the lowest RMSE from all the models for the estimated BPF. From the BPF, analyzing each patient individually, PP estimation could be distinguished in terms of its RMSE which was the lowest amongst the other features.

Besides all the posed comparisons, in table 8 the decisive selecting metrics (mean SCC and mean RMSE, for all patients) for each model were addressed (SCC_1 and $RMSE_1$). M4 had the highest SCC but also the highest RMSE, which is not desirable. Together with the general weak and moderate SCC that are observed in table 7 for patient 3, the mean values SCC_2 and $RMSE_2$, which excluded patient 3, were also calculated. As a result, the metrics' performance increased substantially for all the considered models. Given this inconsistent behaviour from the patient 3, SCC_2 and $RMSE_2$ were taken into account as the decisive factors on the selection of the best performing model. M2 was considered to combine the best SCC_2 and $RMSE_2$ values. Although the best SCC_2 belonged to M4, its $RMSE_2$ was more significant, compared with M2. M6 was also analysed given the implementation's advantage it brings

(compared with M2) where it only depends on PPG based features, dismissing any information from ECG.

Table 8: Mean SCC and Mean RMSE for each one of the seven considered models regarding patients 1,3 and 5 (SCC_1 and $RMSE_1$) and also solely patients 1 and 5 (SCC_2 and $RMSE_2$)

	SCC_1	$RMSE_1$	SCC_2	$RMSE_2$
M1	0.77	11.70	0.88	10.06
M2	0.70	11.31	0.88	9.09
M3	0.56	10.81	0.65	9.94
M4	0.87	21.52	0.91	10.30
M5	0.74	11.92	0.87	10.16
M6	0.72	12.14	0.85	10.25
M7	0.67	12.05	0.86	10.14

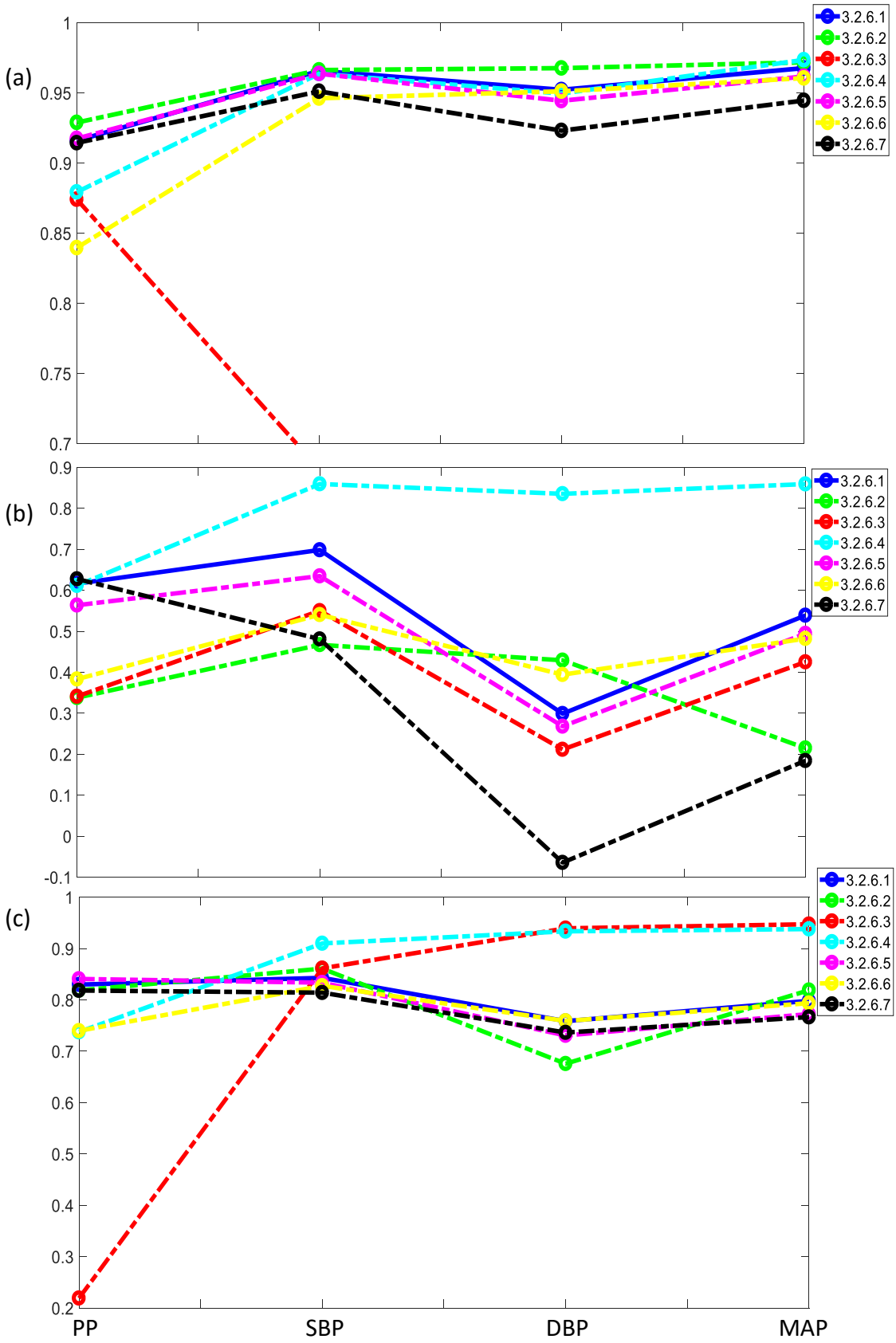

Figure 20: Graphical representation of the resulting *SCC* from the BPF estimation, concerning every considered strategy for patient (a) 1, (b) 3 and (c) 5. Xx-axis: BPF. Yy-axis: *SCC*

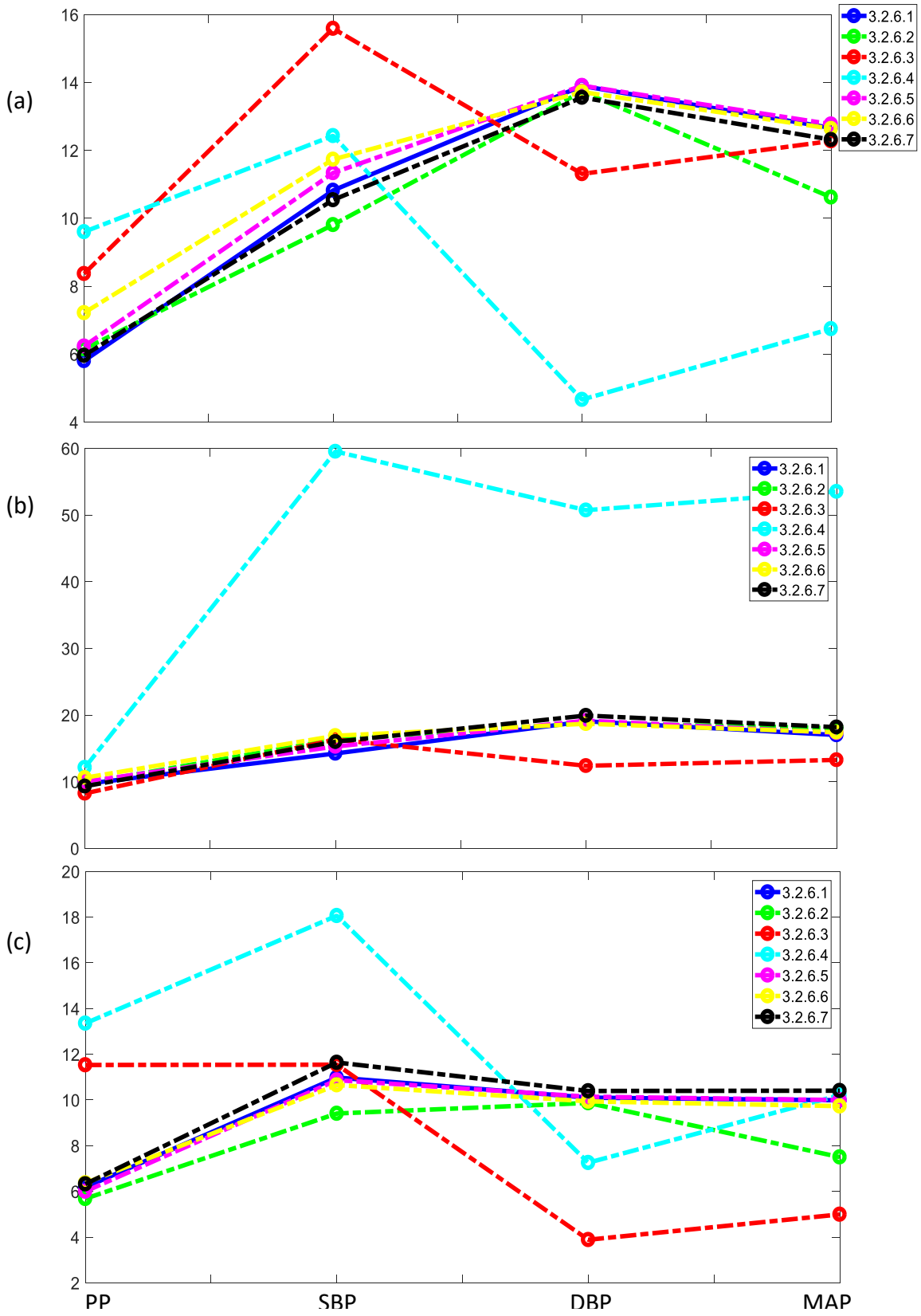

Figure 21: Graphical representation of the resulting RMSE from the BPF estimation, concerning every considered strategy for patient (a) 1, (b) 3 and (c) 5 Xx-axis: BPF; Yy-axis: RMSE

4.7. Models' evaluation within AAMI and BHS protocols

Considering the percentage DIFF for the 3 patients in table 9 and the BHS_{np} requirements, M2 is A graded for PP estimation and C grade for SBP, DBP and MAP estimations. Given the comparison made on table 8, a counter-intuitive better performance was observed for M6 which was A graded for PP estimation, B graded for DBP and MAP estimations and C graded only for SBP estimation. According to BHSnp, the achievement of the grade A or B allows any measuring system to be recommended for clinical use [22]. This means that only SBP could not be effectively measured in M6, while M2 only succeeded to measure PP.

Table 9: Percent DIFF values within the ranges 5, 10 and 15 mmHg using 4970 points (entire biosignals of the 3 patients). M2 in dark grey and M6 in light grey.

	Differences between real and estimated values					
	≤5	≤10	≤15	≤5	≤10	≤15
PP	73	91	98	67	90	97
SBP	48	74	86	42	73	86
DBP	45	79	90	53	83	91
MAP	48	79	90	53	81	90
	M2			M6		

For this data, the exclusion of PAT actually helped to slightly enhance the results of the implemented measuring system, namely for DBP and MAP estimation. Several reasons may account for this observation. One might be related with the selective process which is exerted in the model of M2 that neglects useful information. To explore whether any of the other models could improve the estimation performance, they were also classified according to BHS_{np}. Nevertheless, no significant differences were found. This means that the previously reported varying vascular properties amongst the subjects were suppressed by the other features. This indicates that in future studies, it should be given more relevance to them, starting with $\frac{B}{A}$ due to the reviewed literature and the good reported performance in table 7.

$\overline{DIFF}$ and SD were also determined in order to assess whether the implemented model is within AAMI recommendations. This time, given the results from BHS_{np}, only M6 was evaluated. Firstly, the corresponding Bland-Altman plots were drawn for each feature from BPF in order to allow the inspection the general distribution of DIFF (figue kl). $\overline{DIFF}$ was fixed in zero (solid horizontal line) for every BP feature. This shows the consistency of the bias whose adjustment only requires the subtraction of the $\overline{DIFF}$ from the estimated values. The bias is related with the tendency for one method to exceed the other which is perceived from the estimated $\overline{DIFF}$ and SD [54]. After this operation, and since the $\overline{DIFF}$ values are equal to 0 mmHg, the inspection of the SD values was made. For PP, SBP, DBP and MAP the SD was of 6.48, 11.55, 8.25 and 8.97 mmHg. This means that only PP estimation is approved within AAMI recommendations (SD $\leq$ 8 mmHg), though DBP and MAP estimations associated SD values (of 8.25 and 8.97 mmHg, respectively) were not far from that approval.

From figure 22, the associated variability to the range of BP measurements is noticeable. On one hand, for SBP, DBP and MAP estimations, the spreading out of DIFF values with increasing magnitude is shown, mainly depicted for pressure values associated to hypertension. On the other hand, for PP estimation, a negatively proportional relationship for DIFF values was observed which is related to a proportional error. However, for PP it is observed a lower density of points to contribute to this adverse effect. In general, it is reasonable to agree that these outlying readings were the reason for a worse performance.

Overall, the best BPF to be measured was PP which respected the restrictions from both accepted protocols. Nevertheless, MAP and DBP were accepted according to 1 of the 2 protocols. SBP estimation was not as accurate which implies it might not be the easiest feature to keep track of within the pool of highlighted PPG features.

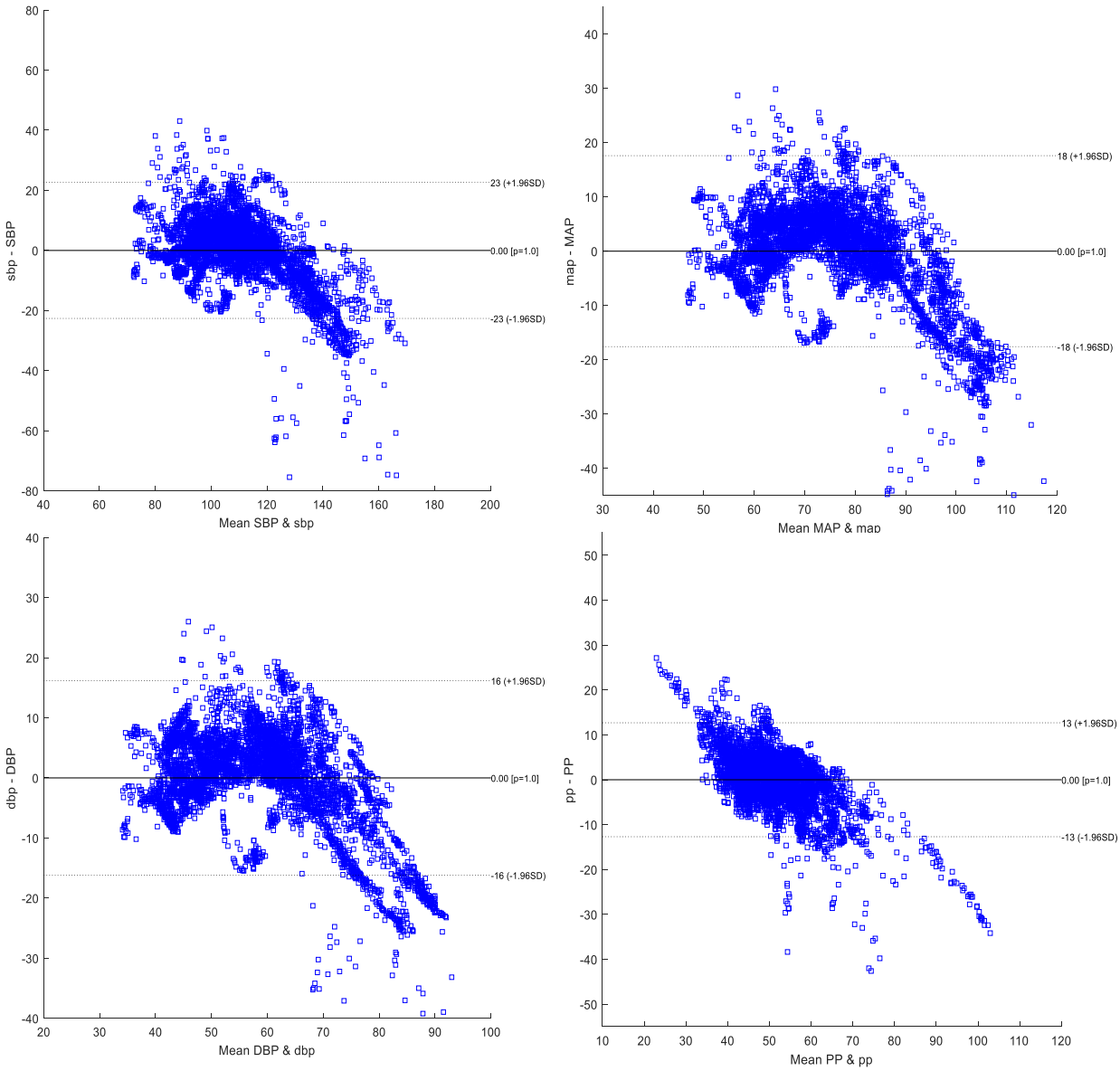

Figure 22: Bland and Altman diagrams of SBP (a), MAP (b), DBP (c), PP (d). The upper-case and lower-case abbreviations of BPF correspond to the real and estimated values, respectively. Dashed horizontal line = mean±1.96*SD. A total number of 4970 samples are here graphically represented (from all patients).

5

Conclusion

The present dissertation has corroborated the strong relationship between PPG and BP features. M2 (which considered only W70b in the training set) was considered the best performing BPF estimation model, in terms of the obtained mean RMSE and SCC, between BP estimated and real measurements, of all patients (9.09 and 0.88, respectively). When validated within BHS protocol, M2 was able to estimate PP according to the imposed requirements (A graded) while M6 (which disregarded the extra usage of ECG sensors) was able to estimate PP, DBP and MAP according to the imposed requirements (graded with A, B, B, respectively). This provides an indication that the PPG considered features in this dissertation might have compensated the exclusion of both PAT features in M6, for this data. However, the small number of patients doesn't allow to state that PAT is not a good marker for BP estimation. Also, the implemented calibration didn't contribute for the improvement of the estimation performance of the studied patients. Despite PP estimation was the only to be validated within the two most recognized standards for evaluating BP measurement automatic systems (AAMI and BHS), DBP and MAP estimations only failed to meet AAMI requirements, though their SD values (of 8.25 and 8.97 mmHg, respectively) weren't much bigger than the imposed SD of 8 mmHg by AAMI. Solely SBP assessment failed to meet any of the imposed criteria.

Further work can be done on testing this system in the context of larger populations. Moreover, the observed heterogeneity of the population has to be addressed towards an improved model and estimation of the BP features. There are many factors that influence the BP waveform, such as sex, heart rate, diabetes hypertension which have already been physiologically interpreted and framed [59,43,51]. In fact, the categorization of people based on standard parameters has already been evaluated. The aforementioned relationship between age and cardiovascular peculiarities with $\frac{B}{A}$ was one of the validated formal findings on this subject [24]. In a similar study, the division of the considered patients in the experiment according to their age allowed a better performance towards BP estimation rather than when no categorization was implied [43]. Visually, BP waveforms were also successfully characterized in healthy aging, according to the corresponding RI [60]. Therefore, future studies on the exploration of such patterns are suggested. These might provide the standard parameters, preferentially extracted from easily measured

biosignals, for the sought categorization. In an equally ambitious perpective, it is suggested further exploration on BP estimation through PPG features which have been positively associated to BP characteristic waveform such as $\frac{B}{A}$ and RI.

References

1) Safety, WHO Patient, and World Health Organization. "WHO guidelines for safe surgery: 2009: safe surgery saves lives." (2009).

2) Dubin, Adrienne E., and Ardem Patapoutian. "Nociceptors: the sensors of the pain pathway." The Journal of clinical investigation 120, no. 11 (2010): 3760.

3) Gruenewald, M., C. Ilies, J. Herz, T. Schoenherr, A. Fudickar, J. Höcker, and B. Bein. "Influence of nociceptive stimulation on analgesia nociception index (ANI) during propofol–remifentanil anaesthesia." British journal of anaesthesia 110, no. 6 (2013): 1024-1030.

4) Rani, D. Devika, and S. S. Harsoor. "Depth of general anaesthesia monitors." Indian journal of anaesthesia 56, no. 5 (2012): 437.

5) Rampil, Ira J. "A primer for EEG signal processing in anesthesia." Anesthesiology: The Journal of the American Society of Anesthesiologists 89, no. 4 (1998): 980-1002.

6) Avramov, Michail N., and Paul F. White. "Methods for monitoring the level of sedation." Critical care clinics 11, no. 4 (1995): 803-826.

7) Jameson, Leslie C., and Tod B. Sloan. "Using EEG to monitor anesthesia drug effects during surgery." Journal of clinical monitoring and computing 20, no. 6 (2006): 445-472.

8) Huiku, M., K. Uutela, M. Van Gils, I. Korhonen, M. Kymäläinen, P. Meriläinen, M. Paloheimo et al. "Assessment of surgical stress during general anaesthesia." British journal of anaesthesia 98, no. 4 (2007): 447-455.

9) Ben-Israel, Nir, Mark Kliger, Galit Zuckerman, Yeshayahu Katz, and Ruth Edry. "Monitoring the nociception level: a multi-parameter approach." Journal of clinical monitoring and computing 27, no. 6 (2013): 659-668.

10) Sinha, Prabhat Kumar, and Thomas Koshy. "Monitoring devices for measuring the depth of anaesthesia-an overview." Indian Journal of Anaesthesia 51, no. 5 (2007): 365.

11) Griffith D, Jones JB. Awareness and memory in anaesthetised patients. Br J Anaesth 1990; 65: 603-7.

12) Sun, S., R. Bezemer, X. Long, J. Muehlsteff, and R. M. Aarts. "Systolic blood pressure estimation using PPG and ECG during physical exercise." Physiological measurement 37, no. 12 (2016): 2154.

13) Jeong, Incheol, Sukhwan Jun, Daeja Um, Joonghwan Oh, and Hyungro Yoon. "Non-invasive estimation of systolic blood pressure and diastolic blood pressure using photoplethysmograph components." Yonsei medical journal 51, no. 3 (2010): 345-353.

14) Elgendi, Mohamed. "On the analysis of fingertip photoplethysmogram signals." Current cardiology reviews 8, no. 1 (2012): 14-25.

15) Shelley, Kirk H. "Photoplethysmography: beyond the calculation of arterial oxygen saturation and heart rate." Anesthesia & Analgesia 105, no. 6 (2007): S31-S36.

16) Rani, D. Devika, and S. S. Harsoor. "Depth of general anaesthesia monitors." Indian journal of anaesthesia 56, no. 5 (2012): 437.

17) Castro, Ana Isabel Rodrigues. "Nociception level during anaesthesia: Analysis and control." PhD diss., Universidade do Porto (Portugal), 2011.

18) Neukirchen, Martin, and Peter Kienbaum. "Sympathetic Nervous SystemEvaluation and Importance for Clinical General Anesthesia." The Journal of the American Society of Anesthesiologists 109, no. 6 (2008): 1113-1131.

19) Chen, W., T. Kobayashi, S. Ichikawa, Y. Takeuchi, and T. Togawa. "Continuous estimation of systolic blood pressure using the pulse arrival time and intermittent calibration." Medical and Biological Engineering and Computing 38, no. 5 (2000): 569-574.

20) Parati, Gianfranco, and Mariaconsuelo Valentini. "Prognostic relevance of blood pressure variability." Hypertension 47, no. 2 (2006): 137-138.

21) McCombie, Devin B., Andrew T. Reisner, and H. Harry Asada. "Adaptive blood pressure estimation from wearable PPG sensors using peripheral artery pulse wave velocity measurements and multi-channel blind identification of local arterial dynamics." In Engineering in Medicine and Biology Society, 2006. EMBS'06. 28th Annual International Conference of the IEEE, pp. 3521-3524. IEEE, 2006.

22) O'brien, Eoin, James Petrie, William Littler, Michael de Swiet, Paul L. Padfield, Kevin O'malley, Michael Jamieson, Douglas Altman, Martin Bland, and Neil Atkins. "The British Hypertension Society protocol for the evaluation of automated and semi-automated blood pressure measuring devices with special reference to ambulatory systems." Journal of hypertension 8, no. 7 (1990): 607-619.

23) Lee, Han-Wook, Ju-Won Lee, Won-Geun Jung, and Gun-Ki Lee. "The periodic moving average filter for removing motion artifacts from PPG signals." International Journal of Control, Automation, and Systems 5, no. 6 (2007): 701-706.

24) Hashimoto, Junichiro, Kenichi Chonan, Yohei Aoki, Takuya Nishimura, Takayoshi Ohkubo, Atsushi Hozawa, Michiko Suzuki et al. "Pulse wave velocity and the second derivative of the finger photoplethysmogram in treated hypertensive patients: their relationship and associating factors." Journal of hypertension 20, no. 12 (2002): 2415-2422.

25) Madhav, K. Venu, M. Raghu Ram, E. Hari Krishna, Nagarjuna Reddy Komalla, and K. Ashoka Reddy. "Estimation of respiration rate from ECG, BP and PPG signals using empirical mode decomposition." In *Instrumentation and Measurement Technology Conference (I2MTC), 2011 IEEE*, pp. 1-4. IEEE, 2011.

26) Farina, Dario, Mauro Fosci, and Roberto Merletti. "Motor unit recruitment strategies investigated by surface EMG variables." Journal of Applied Physiology 92, no. 1 (2002): 235-247.

27) Bruce, J., E. M. Russell, J. Mollison, and Z. H. Krukowski. The measurement and monitoring of surgical adverse events. Health Technology Assessment Programme, 2001.

28) Storm, Hanne. "Changes in skin conductance as a tool to monitor nociceptive stimulation and pain." Current Opinion in Anesthesiology 21, no. 6 (2008): 796-804.

29) Augusto, J-F., J-L. Teboul, P. Radermacher, and P. Asfar. "Interpretation of blood pressure signal: physiological bases, clinical relevance, and objectives during shock states." Intensive care medicine 37, no. 3 (2011): 411-419.

30) Kelley, Scott D., and Michael AE Ramsay. "Respiratory rate monitoring: characterizing performance for emerging technologies." (2014): 1246-1248.

31) PS, Mr Kiran Balaji, and Mr Anand Jatti. "PPG Signal for Extraction of Respiratory Activity and HR Monitoring of CHF Patients." International Journal 4, no. 1 (2014).

32) Brouse, Chris J. "Monitoring nociception during general anesthesia with heart rate variability." PhD diss., University of British Columbia, 2015.

33) Cividjian, A., J. Y. Martinez, E. Combourieu, P. Precloux, A. M. Beraud, Y. Rochette, M. Cler, L. Bourdon, J. Escarment, and L. Quintin. "Beat-by-beat cardiovascular index to predict unexpected intraoperative movement in anesthetized

unparalyzed patients: a retrospective analysis." Journal of clinical monitoring and computing 21, no. 2 (2007): 91.

34) Conway, Aaron, and Joanna Sutherland. "Depth of anaesthesia monitoring during procedural sedation and analgesia: A systematic review and meta-analysis." International journal of nursing studies 63 (2016): 201-212.

35) Scheer, Bernd Volker, Azriel Perel, and Ulrich J. Pfeiffer. "Clinical review: complications and risk factors of peripheral arterial catheters used for haemodynamic monitoring in anaesthesia and intensive care medicine." Critical Care 6, no. 3 (2002): 199.

36) Warren, David K., Wasim W. Quadir, Christopher S. Hollenbeak, Alexis M. Elward, Michael J. Cox, and Victoria J. Fraser. "Attributable cost of catheter-associated bloodstream infections among intensive care patients in a nonteaching hospital." Critical care medicine 34, no. 8 (2006): 2084-2089.

37) Bonhomme, V., M. Jeanne, E. Boselli, M. Gruenewald, R. Logier, and P. Richebé. "Physiological signal processing for individualized anti-nociception management during general anesthesia: a review." Yearbook of medical informatics 10, no. 1 (2015): 95.

38) Jeanne, M., R. Logier, J. De Jonckheere, and B. Tavernier. "Validation of a graphic measurement of heart rate variability to assess analgesia/nociception balance during general anesthesia." In Engineering in Medicine and Biology Society, 2009. EMBC 2009. Annual International Conference of the IEEE, pp. 1840-1843. IEEE, 2009.

39) Malamed, Stanley F. Sedation-E-Book: A Guide to Patient Management. Elsevier Health Sciences, 2017.

40) Braithwaite, Jason J., Derrick G. Watson, Robert Jones, and Mickey Rowe. "A guide for analysing electrodermal activity (EDA) & skin conductance responses (SCRs) for psychological experiments." Psychophysiology 49 (2013): 1017-1034.

41) Martinez, Jean Yves, Pierre François Wey, Christophe Lions, Andrei Cividjian, Muriel Rabilloud, Alvine Bissery, Lionel Bourdon, Marc Puidupin, Jacques Escarment, and Luc Quintin. "A beat-by-beat cardiovascular index, CARDEAN: a prospective randomized assessment of its utility for the reduction of movement during colonoscopy." Anesthesia & Analgesia 110, no. 3 (2010): 765-772.

42) Ruiz-Rodríguez, Juan C., Adolf Ruiz-Sanmartín, Vicent Ribas, Jesús Caballero, Alejandra García-Roche, Jordi Riera, Xavier Nuvials et al. "Innovative continuous non-

invasive cuffless blood pressure monitoring based on photoplethysmography technology." Intensive care medicine 39, no. 9 (2013): 1618-1625.

43) Suzuki, Satomi, and Koji Oguri. "Cuffless and non-invasive systolic blood pressure estimation for aged class by using a photoplethysmograph." In Engineering in Medicine and Biology Society, 2008. EMBS 2008. 30th Annual International Conference of the IEEE, pp. 1327-1330. IEEE, 2008.

44) Baek, Hyun Jae, Ko Keun Kim, Jung Soo Kim, Boreom Lee, and Kwang Suk Park. "Enhancing the estimation of blood pressure using pulse arrival time and two confounding factors." Physiological measurement 31, no. 2 (2009): 145.

45) Muehlsteff, J., X. A. Aubert, and G. Morren. "Continuous cuff-less blood pressure monitoring based on the pulse arrival time approach: The impact of posture." In *Engineering in Medicine and Biology Society, 2008. EMBS 2008. 30th Annual International Conference of the IEEE*, pp. 1691-1694. IEEE, 2008.

46) Couceiro, Ricardo, Paulo Carvalho, R. P. Paiva, Jens Muehlsteff, Jorge Henriques, Volker Schulze, Anita Ritz, Malte Kelm, and Christian Meyer. "Characterization of surrogate parameters for blood pressure regulation in neurally-mediated syncope." In *Engineering in Medicine and Biology Society (EMBC), 2013 35th Annual International Conference of the IEEE*, pp. 5381-5385. IEEE, 2013.

47) Jeanne, M., R. Logier, J. De Jonckheere, and B. Tavernier. "Validation of a graphic measurement of heart rate variability to assess analgesia/nociception balance during general anesthesia." In Engineering in Medicine and Biology Society, 2009. EMBC 2009. Annual International Conference of the IEEE, pp. 1840-1843. IEEE, 2009.

48) Jeanne, Mathieu, Michel Delecroix, Julien De Jonckheere, Abdel Keribedj, Régis Logier, and Benoît Tavernier. "Variations of the analgesia nociception index during propofol anesthesia for total knee replacement." *The Clinical journal of pain* 30, no. 12 (2014): 1084-1088.

49) Nguyen, Tuan Ngoc. "An algorithm for extracting the PPG Baseline Drift in real-time." (2016).

50) Kaufmann, S., A. Malhotra, G. Ardelt, N. Hunsche, K. Breßlein, R. Kusche, and M. Ryschka. "A system for in-ear pulse wave measurements." PAT 4 (2014): 6.

51) Townsend, Raymond R., Clive Rosendorff, Wilmer W. Nichols, David G. Edwards, Julio A. Chirinos, Bo Fernhall, and William C. Cushman. "American Society

of Hypertension position paper: central blood pressure waveforms in health and disease." (2016): 22-33.

52) Mukaka, Mavuto M. "A guide to appropriate use of correlation coefficient in medical research." Malawi Medical Journal 24, no. 3 (2012): 69-71.

53) Paleologu, Constantin, Jacob Benesty, and Silviu Ciochină. "A practical variable forgetting factor recursive least-squares algorithm." In Electronics and Telecommunications (ISETC), 2014 11th International Symposium on, pp. 1-4. IEEE, 2014.

54) Bland, J. Martin, and Douglas G. Altman. "Measuring agreement in method comparison studies." Statistical methods in medical research 8, no. 2 (1999): 135-160.

55) Clifford, Gari D., Daniel J. Scott, and Mauricio Villarroel. "User guide and documentation for the MIMIC II database." MIMIC-II database version 2, no. 95 (2009).

56) Elgendi, Mohamed, Ian Norton, Matt Brearley, Derek Abbott, and Dale Schuurmans. "Detection of a and b waves in the acceleration photoplethysmogram." *Biomedical engineering online* 13, no. 1 (2014): 139.

57) Elgendi, Mohamed. "Detection of c, d, and e waves in the acceleration photoplethysmogram." *Computer methods and programs in biomedicine* 117, no. 2 (2014): 125-136.

58) Wang, L., Emma Pickwell-MacPherson, Y. P. Liang, and Yuan Ting Zhang. "Noninvasive cardiac output estimation using a novel photoplethysmogram index." In Engineering in Medicine and Biology Society, 2009. EMBC 2009. Annual International Conference of the IEEE, pp. 1746-1749. IEEE, 2009.

59) Gibson, Stephen J., and Michael Farrell. "A review of age differences in the neurophysiology of nociception and the perceptual experience of pain." The Clinical journal of pain 20, no. 4 (2004): 227-239.

60) Murgo, JOSEPH P., N. I. C. O. Westerhof, John P. Giolma, and Stephen A. Altobelli. "Aortic input impedance in normal man: relationship to pressure wave forms." Circulation 62, no. 1 (1980): 105-116.

61) "Nihon Kohden Dominating High-Tech Asia-Pacific Patient Monitoring Market, Chased by Philips Healthcare, GE Healthcare, and Fukuda Denshi." IData Research. May 26, 2017. Accessed September 12, 2017. https://idataresearch.com/nihon-kohden-dominating-high-tech-asia-pacific-patient-monitoring-market-chased-philips-healthcare-ge-healthcare-fukuda-denshi/.